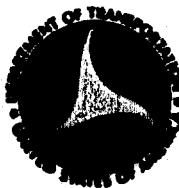


AD726249

STUDY OF VISIBLE EXHAUST SMOKE FROM AIRCRAFT JET ENGINES

John Stockham and Howard Betz
IIT Research Institute
10 West 35th Street, Chicago, Illinois 60616



JUNE 1971

FINAL REPORT

DDC
RECEIVED
JUL 16 1971
REGULATORY
C

Availability is unlimited. Document may be released to the National Technical Information Service, Springfield, Virginia 22151, for sale to the public.

Prepared for

**DEPARTMENT OF TRANSPORTATION
FEDERAL AVIATION ADMINISTRATION**

Systems Research & Development Service

Washington D. C., 20590

ACCESSION FOR	
CFSTI	WHITE SEC. <input checked="" type="checkbox"/>
DDC	BUFF SEC. <input type="checkbox"/>
UNANNOUNCED	<input type="checkbox"/>
JUSTIFICATION	<input type="checkbox"/>
BY	
DISTRIBUTION AVAILABILITY	
DIST.	AVAIL. and/or SPECIAL
A	

The contents of this report reflect the views of the contractor, which is responsible for the facts and the accuracy of the data presented herein, and do not necessarily reflect the official views or policy of the FAA or Department of Transportation. This report does not constitute a standard, specification, or regulation.

1. Report No. FAA-RD-71-22	2. Government Accession No.	3. Recipient's Catalog No.	
4. Title and Subtitle Study of Visible Exhaust Smoke From Aircraft Jet Engines		5. Report Date June 1971	
		6. Performing Organization Code	
7. Author(s) John Stockham and Howard Betz		8. Performing Organization Report No. FAA-NA-71-24	
9. Performing Organization Name and Address IIT Research Institute 10 West 35th Street Chicago, Illinois 60616		10. Work Unit No.	
		11. Contract or Grant No. (502-306-02X) DOT-FA69WA-2208	
12. Sponsoring Agency Name and Address Federal Aviation Administration Systems Research & Development Service Washington, D.C. 20590 & National Air Pollution Control Administration		13. Type of Report and Period Covered Final Report	
		14. Sponsoring Agency Code	
15. Supplementary Notes NONE Details of illustrations in this document may be better studied on microfiche			
16. Abstract The objective of this study was to relate the visibility of inflight jet exhaust to the SAE smoke number. A method based on photographic photometry was developed for measuring the optical density of smoke plumes. This method was related to visibility and to the smoke number through transmissometer measurements and visibility theory. A portable transmissometer, capable of operating over a wide range of optical path lengths and under varying ambient light conditions was fabricated for use on this study. The mathematical expression relating the transmission measurements to the smoke number was derived. Liminal visibility requirements of smoke trails, developed from light scattering theory, correlated with actual visual observations and the transmissometer and photometry measurements. Test results, with the engines investigated, indicate that SAE smoke numbers below 23 were associated with invisible exhaust plumes. Samples of the exhaust smoke showed the particles to be composed of lacy agglomerates. At the nozzle, the geometric median particle diameter was 0.052 μm . At a distance of 10 nozzle diameters the geometric median particle diameter was 0.13 μm at cruise condition.			
17. Key Words Pollution Smoke Jet Aircraft		18. Distribution Statement Availability is unlimited. Document may be released to the National Technical Information Service, Springfield, Virginia 22151, for sale to the public.	
19. Security Classif. (of this report) Unclassified	20. Security Classif. (of this page) Unclassified	21. No. of Pages 75	22. Price

PREFACE

This report was prepared by the IIT Research Institute for the Federal Aviation Administration and the National Air Pollution Control Administration. The work effort was a part of a program of the Aircraft Division, Systems Research and Development Service, Federal Aviation Administration, and the Division of Motor Vehicle Research and Development, National Air Pollution Control Administration.

The work was administered under the direction of Mr. G. R. Slusher who served as project manager. Provision of the facilities, conduct of the tests and collection and reduction of the data for the SAE smoke numbers were furnished by the Propulsion Section, Aircraft Branch, Test and Evaluation Division, National Aviation Facilities Experimental Center, Atlantic City, New Jersey.

TABLE OF CONTENTS

	Page
INTRODUCTION	1
(1.) Purpose	1
(2.) Background	1
DISCUSSION	3
(3.) Modeling Studies	3
(3.1) Light-Scattering Theory	3
(3.2) Visibility Requirements	3
(3.3) Theory Relating the Smoke Number and Optical Transmission of Jet Exhaust Plumes	9
(3.3.1) Reflectivity of Soot Deposition Filter Paper	11
(3.3.2) Optical Transmission of Smoke Plumes	12
(3.3.3) Relating D_R to D_T and Operating Parameters	13
(3.3.4) Relating Smoke Number to Filter Density	15
(4.) Static Tests of Engines and Aircraft	16
(4.1) J-57-P-37A Engine Mounted in the Test Cell	16
(4.2) Light Transmission of J-57 Engine Exhaust for Various Path Lengths	17
(4.3) JT-12-6 Engine Mounted in Wind Tunnel	20
(4.4) Tied-Down Aircraft Tests	20
(4.4.1) F-100 Single-Engine Aircraft	20
(4.4.2) Convair 880 Aircraft	24
(4.4.3) Multiple Engines of Convair 880 Aircraft	24
(4.4.4) Lockheed Jetstar Aircraft	30
(4.5) Discussion and Summary of Results of Static Engine and Aircraft Tests	30
(5.) In-Flight Observations	32
(5.1) Flights Evaluated at NAFEC	32
(5.1.1) F-100 and F-105 Aircraft In-Flight Tests	32
(5.1.2) Convair 880 Aircraft In-Flight Tests	39
(5.1.3) Lockheed Jetstar Aircraft In-Flight Tests	39

TABLE OF CONTENTS (Continued)

	Page
(5.2) Observations of Aircraft In-Flight at Chicago O'Hare Airport	39
(5.3) Discussion and Summary of In-Flight Tests	39
CONCLUSIONS	45
REFERENCES	46
APPENDIX A Transmissometer (4 pages)	1-1
APPENDIX B Photographic Instrumentation (7 pages)	2-1
APPENDIX C Sampling Jet Exhaust for Particular Matter (4 pages)	3-1
APPENDIX D SAE Standard Method for Smoke Measurements (3 pages).	4-1

LIST OF ILLUSTRATIONS

Figure		Page
1	Visibility of Line Targets	8
2	Electron Photomicrographs of Jet Engine Exhaust Particles	10
3	Smoke Instrumentation	23
4	Microdensitometer Trace of Number 1 Engine of Convair 880 Aircraft	26
5	Number 1 Engine of the Convair 880 Aircraft	27
6	Microdensitometer Traces from Tied-Down Convair 880 Aircraft	28
7	Plot of Smoke Number vs Optical Transmission	33
8	NAFEC/Atlantic City Airport	35
9	Photographs of F-100 and Convair 880 Aircraft In Flight	36
10	Photographs of Jet Exhaust Trails During Takeoff at O'Hare Airport	43
1.1	Transmissometer	1-2
1.2	Optical Schematic	1-3
2.1	Typical H & D Curve	2-3
2.2	Illustration of Use of Photographic Photometry	2-6
3.1	Exhaust Particulate Sampling Apparatus	3-2
3.2	IITRI Smoke Sampler in the Engine Test Cell	3-3
4.1	F-100 Aircraft with Sampling Probes	4-2
4.2	General Electric Smoke Sampling Console	4-3

LIST OF TABLES

Table		Page
1	Relationship Between Ringelmann Number, Light Transmission, and Particle Concentration of Turbojet Engine Exhaust	5
2	Particle Size Distribution of Exhaust from J-57 Engine	7
3	Smoke Numbers and Transmission Data of Jet Smoke - J-57 Engine	18
4	Light Transmission as a Function of Path Length	19
5	Smoke Numbers and Transmission Data of Jet Smoke-JT-12-6 Engine Mounted in Wind Tunnel	21
6	Smoke Quality from a Tied-Down F-100 Aircraft	22
7	Smoke Quality from the Number 1 Engine of a Tied-Down CV-880 Aircraft	25
8	CV-880 Aircraft Tied-Down Multiple Engine Observation	29
9	Smoke Numbers from the Number 4 Engine of a Tied-Down Jetstar Aircraft	31
10	Summary of Smoke Number and Transmission for Static Tests	34
11	Observations on the F-100 Aircraft In-Flight at NAFEC	37
12	Observations on the F-105 Aircraft In-Flight at NAFEC	38
13	Observations on the Convair 880 Aircraft In-Flight at NAFEC	40
14	Photographic Measurement of Jet Smoke Trails from Aircraft In-Flight at O'Hare Airport and Visual Estimates of Transmission	41
3.1	Size Distribution and Concentration of Exhaust Particles - Royco Particle Counter-J-57-P-37A	3-5
3.2	Size Distribution and Concentration of Exhaust Particles - Royco Particle Counter JT12-6	3-6

INTRODUCTION

(1.) Purpose

The purpose of this research program was to develop techniques for the objective determination of visibility of jet exhaust smoke and to relate these techniques to the smoke number obtained for engines mounted in test cells. Use of the established relationships should enable the prediction of in-flight visibility of smoke trails from test cell data. A theoretical model of smoke trail visibility using the physical and optical properties of the smoke particles was included in the research effort.

(2.) Background

Smoke trails from aircraft turbine engines are a symbol of air pollution. Elimination of these smoke trails would erase a source of pollution complaints and improve visibility in and around jetports. Engine smoke is currently determined by a filter stain technique described by **The Society of Automotive Engineers (Reference 1)**. The results are expressed as a numerical value known as the **SAE smoke number**. This technique is applied to engine test cell operations. A need exists for an objective measure of the visibility of smoke trails of aircraft in-flight, especially at take-off and approach power conditions, and to relate this measurement to the SAE smoke number. The only currently accepted method for specifying the visual quality of smoke trails from aircraft in-flight is the Ringelmann method (Reference 2). This is a subjective measurement. Results are highly dependent upon the conditions under which the measurements are performed (Reference 3).

Two techniques were developed to accomplish the objectives of this program. The first involved a transmissometer to measure the light attenuation of the smoke, and the second was photographic photometry. A special two-path transmissometer was developed for measuring the optical attenuation of smoke from test cell engines and engines of tied-down aircraft. The transmissometer is described in Appendix A. Photographic photometry was developed for evaluating the visibility of smoke from aircraft in-flight and from tied-down aircraft. This procedure is described in Appendix B.

The following measurements were made during this program:

- (1) Photographic photometry measurements and Ringelmann observations of in-flight jet aircraft exhaust were made at Chicago's O'Hare Airport and at the National Aviation Facilities Experimental Center (NAFEC), Atlantic City, New Jersey. Aircraft studied included a variety of commercial jets and the F-100, F-105, CV-880, and the Lockheed Jetstar.
- (2) Photographic photometry and transmissometer measurements, Ringelmann observations, and the filter stain technique were all used to evaluate smoke emissions from tied-down aircraft at NAFEC. Aircraft used were the F-100, CV-880, and the Jetstar. NAFEC personnel obtained the SAE smoke numbers.
- (3) Transmissometer measurements and SAE smoke numbers were made on test engines. One, a J-57 engine, was mounted on a static, sea-level, open-air test stand; the other, a JT-12 engine was mounted as a flight installation in a test wind tunnel. Samples of exhaust smoke were obtained during these tests using a specially constructed sampling rig described in Appendix C.

Quantitative data from the instrumental techniques were correlated with the subjective Ringelmann observations and visibility theory. The correlation established the relationship between the smoke number, the optical attenuation, photographic photometry, and the visual appearance of jet smoke.

DISCUSSION

(3.) Modeling Studies

(3.1) Light-Scattering Theory

The visibility of a smoke plume is a function of the optical and physical properties of the particles comprising the plume, the width of the plume, and the contrast between the plume and its background.

Where a smoke particle is small in relation to the wavelength of incident light, the total attenuation of light, i.e., extinction, E , is given by the expression:

$$E = \frac{24 \alpha n^2 k}{(n^2 + n^2 k^2) + 4(n^2 - n^2 k^2 - 1)} \quad (1)$$

where,

$$\alpha = \frac{2\pi r}{\lambda}$$

λ = wavelength of light, μm

r = particle radius, μm

n, k = functions of the refractive index, η , of the particle.

The refractive index, η , of a particle is a complex number when the particle both absorbs and scatters the incident light. In these instances, the refractive index is equal to $n(1 - ik)$, where n is the coefficient that defines the scattered light and nk the coefficient that defines the absorbed light. The term i is the operator $\sqrt{-1}$. The complex refractive index of carbon, the major particulate component of turbojet engine exhaust (Reference 4), for incident light of wavelength $0.490 \mu\text{m}$ is $1.59 (1 - 1.05i)$. Thus, $n = 1.59$ and $k = 1.05$.

The extinction of light is due to two separate and distinct phenomena; light scattering, S , and light absorption, A . The phenomena are defined as follows:

$$S = \frac{8 \alpha^4}{3} \left| \frac{\eta^2 - 1}{\eta^2 + 2} \right|^2 \quad (2)$$

$$A = E - S$$

Substituting the best available information into Equations (1) and (2), the following values for E, S, and A result:

$$E = 0.9$$

$$S = 0.1$$

$$A = 0.8$$

Thus, the extinction of light by turbojet engine smoke is due to 11% scattering of light and 89% absorption of light.

The attenuation of light by a smoke cloud, where the cloud is so diffuse that complications due to particle interactions are not encountered, is given by the expression:

$$I = I_0 e^{-\pi r^2 C L E} \quad (3)$$

where,

I_0 = the intensity of the incident light

I = the intensity of the transmitted light

C = number concentration of smoke particles

E = extinction coefficient

r = particle radius

L = depth of cloud intervening between I_0 and I .

The ratio I/I_0 is the transmission, T , of light through the smoke.

Thus,

$$2.303 \log T = -\pi r^2 C L E \quad (4)$$

Equation (4) illustrates the dependence of light transmittance through a smoke plume on the length of the viewing path. Thus, the position of the observer in relation to the smoke plume is important to plume visibility.

If the path length, the particle size, and the extinction coefficient are known, it is possible to calculate the number of particles per unit volume of gas that will produce various levels of light attenuation. The data in Table 1 is an example. The path length chosen is the diameter of the J-57

TABLE 1

RELATIONSHIP BETWEEN RINGELMANN NUMBER,
LIGHT TRANSMISSION, AND PARTICLE
CONCENTRATION OF TURBOJET ENGINE EXHAUST

Percent Transmission	Ringelmann Number	Particle Concentration at Engine Nozzle Millions of Particles/cm ³ (1)
98	--	17
95	1/4	50
90	1/2	100
80	1	
60	2	
40	3	
20	4	

(1) Particle concentration data is calculated from equation 4 using a path length of 56 cm and a particle size radius of 0.026 μ m. The path length is the nozzle diameter of the J-57 engine and the particle size is the geometric median particle radius of the exhaust particles at the nozzle under cruise conditions, Table 2.

turbojet engine exhaust nozzle, 56 cm. The geometric median particle diameter of exhaust smoke at the nozzle of the J-57 engine is 0.052 μm , Table 2. The data in Table 1 show that particle concentrations of 1×10^8 particles/cm³ correspond to transmission values of 90% or an equivalent Ringelmann number of 1/2.

(3.2) Visibility Requirements

The visibility requirements for jet smoke trails is similar to those of line targets such as wires, poles, and antennas. Two basic factors are involved in line target visibility. The target must be wide enough to be resolved by the unaided eye and must have sufficient contrast from the background to be distinguished. Tests by Douglas (Reference 5) show flagpoles and radio towers can be resolved if the angle subtended at the eye of the viewer is greater than 3 or 4 sec. of arc. Assuming a nondiffusing smoke track and no attenuation by the intervening atmosphere, a 2 ft. smoke track could be seen at a distance of 20 miles. Obviously, the angle subtended is not a factor limiting the visibility of jet smoke trails. The relationship between angle subtended and contrast is shown in Figure 1. These data (Reference 6) were developed in the IITRI laboratory under ideal conditions; a black line target (contrast = -1) subtending only 0.6 sec. of arc was visible.

Contrast, C_p , between a smoke plume of luminance, B_p , viewed against an extended background of luminance B_b , is given by the expression:

$$C_p = \frac{B_p - B_b}{B_b} \quad (5)$$

From this equation, a totally light absorbing line target has a contrast of -1 and a black smoke plume will have a contrast ranging from 0 to -1 depending on the amount of background light transmitted through the plume. For a plume that scatters a negligible amount of light such as a carbon particle smoke (Reference 7)

$$C_p = T - 1 \quad (6)$$

where T is the transmission.

TABLE 2

PARTICLE SIZE DISTRIBUTIONS OF EXHAUST
FROM THE J-57 ENGINE (1)

Sampler Location, Engine Diameters from Engine Nozzle.	Engine Thrust Setting	Particle Size Distribution	
		Geometric Median Dia. $\mu\text{m } d_g$	Geometric Standard Devia- tion σ_g
0	Approach	---	---
	75% Norm.	0.053	1.63
	Cruise	0.052	1.46
2-1/2	Approach	0.084	1.33
	75% Norm.	0.084	1.40
	Cruise	0.076	1.51
10	Approach	0.096	1.38
	75% Norm.	---	---
	Cruise	0.13	1.40

(1) Data obtained from electron microscope samples collected by the IITRI sampler described in Appendix C.

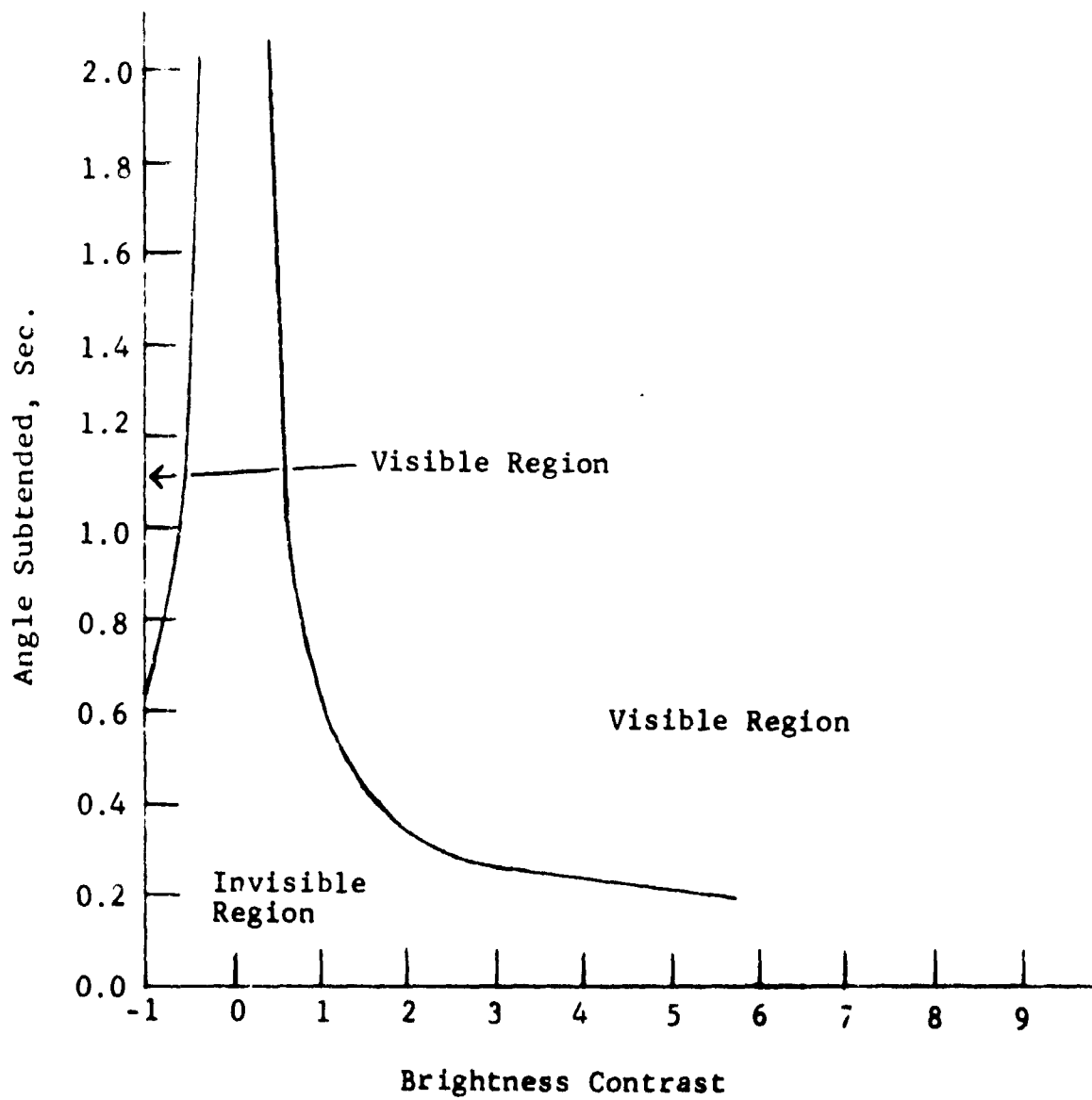


FIGURE 1. VISIBILITY OF LINE TARGETS.

Middleton (Reference 8) discusses the liminal contrast for visibility of a variety of target shapes, sizes, and luminance levels. For targets and luminance levels that approach conditions under which jet engine exhaust plumes are usually viewed the liminal contrast ranges from about 1 to 5%. The visual range of objects in natural light is usually based on the assumption that the liminal contrast is 2%. On this basis, the liminal contrast value of 2% was selected for jet exhaust trails. Substituting 2% into Equation (6) indicates that jet smoke with transmission values of 98% or higher will be invisible.

In conclusion, the modeling studies show that carbon smokes attenuate light mainly by absorption. This factor permits the use of a simple expression to relate contrast and transmission measurements to liminal visibility. This relationship indicates that jet smoke must transmit more than 98% of the incident light to be invisible. Observing the J-57 engine at the nozzle and perpendicular to the exhaust flow, theory predicts that a smoke with a 98% transmission will have a particle concentration of 1.7×10^7 particles/cm³.

The mass concentration of the smoke particles can be computed from number concentration data if the particle density is known. Because of the lacy agglomerated structure of turbojet exhaust particles, as shown in Figure 2, handbook densities cannot be used. If the value of 0.04 g/cm³ reported by Horvath and Charlson (Reference 9) for carbon flocs is used, the mass concentration of the smoke producing a transmitted value of 98% is 0.05 mg/m³. Values found in the literature for exhaust particulates are 36 mg/m³ for a PW-JT8D turbofan engine (Reference 10) and 0.5 and 27.0 mg/m³ for an unstated turbojet engine at approach and takeoff power. (Reference 11)

(3.3) Theory Relating the Smoke Number and Optical Transmission of Jet Exhaust Plumes

It is the purpose of this theoretical analysis to relate the SAE smoke number, the mass flow of an engine, and the dimensions of the nozzle, to the optical attenuation of the smoke plume. The first relationship considered is the effect of particle concentration in the exhaust gas on the staining of the filter paper.



at engine nozzle



2-1/2 nozzle diameters from the engine nozzle



NOT REPRODUCIBLE

10 nozzle diameters from engine nozzle

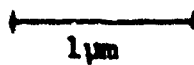


FIGURE 2. ELECTRON PHOTOMICROGRAPHS OF JET ENGINE EXHAUST PARTICLES. J57 ENGINE AT CRUISE.

(3.3.1) Reflectivity of Soot Deposit on Filter Paper

The reflectivity of soot deposit on filter paper may be represented by:

$$I_R = I_o 10^{-K_1 \left(\frac{mQ}{a}\right)^b} \quad (7)$$

where,

I_o = incident light flux

I_R = reflected light flux

m = total mass of gas through the filter

Q = number of particles per unit mass of gas

K_1 = specific attenuation coefficient

a = area of filter paper

b = a number expressing the exponential retention of the filter.

Equation (7) can be restated as:

$$R = \frac{I_R}{I_o} = 10^{-K_1 \left(\frac{mQ}{a}\right)^b} \quad (8)$$

where,

R = absolute reflectivity of the stained spot.

Taking the logarithm of Equation (8) gives:

$$\log_{10} \frac{1}{R} = D_R = K_1 \left(\frac{mQ}{a}\right)^b \quad (9)$$

where D_R is the optical reflection density of the soot deposit.

The validity of this equation may be tested as follows:

Taking the logarithm of Equation (9) we have:

$$\log D_R = b(\log m + \log Q - \log a) + \log K_1 \quad (10)$$

In a given smoke sampling system, the area, a , of the filter and K_1 are constants.

Equation (10) shows that if Q is constant at a given power setting and different masses of gas are filtered, a straight line will result when $\log D_R$ is plotted against $\log m$. The slope of this line will be b . If the power setting is changed, resulting in a different value of Q , another straight line with slope b will result, providing Q remains constant as m is varied. Data for a variety of power settings, therefore, yield a family of parallel straight lines. These lines are offset because of the different particle concentrations, Q , produced at the different power settings. Plots of this type (Reference 12) give a series of parallel straight lines. Data presented in Reference 13 were replotted and resulted in parallel straight lines for approach, cruise and takeoff power. (The line for idle was poorly defined by the data points and appeared to have a slightly different slope. This is not surprising since the smoke numbers for this low power setting are less accurate.) The importance of the relationship is that the slope of the lines is dependent on the filtering characteristics of the filter. Thus, the filter must be specified. Changes in filter specifications will be difficult to accommodate.

(3.3.2) Optical Transmission of Smoke Plume

The transmission of light through a smoke cloud may be represented by the expression:

$$I_T = I_O 10^{-C L K_2} \quad (11)$$

where,

I_O = incident flux

I_T = transmitted flux

K_2 = specific absorption coefficient

L = optical path length

C = concentration of particles/unit volume of gas in the plume.

Equation (11) may be rewritten as:

$$T = \frac{I_T}{I_O} = 10^{-C L K_2} \quad (12)$$

where,

T = transmission

or:

$$\log_{10} \frac{1}{T} = D_T = C L K_2 \quad (13)$$

where D_T is the optical transmission density of the plume. Equations (12) and (13) are universally accepted expressions and need no test for validity.

(3.3.3) Relating D_R to D_T and Operating Parameters

Neither Equation (9) nor Equation (13) are particularly useful for the study of engine exhaust because they contain the quantities Q and C. Neither of these expressions are measured directly by the filter stain technique or by the transmissometer. However, the reflection density of the filter stain can be related to the transmission density of the plume at the engine nozzle through the use of engine parameters and measured values. Thus, theory may be tested by experimentation.

If each unit mass of gas and unit volume of gas issuing from the nozzle of an engine at fixed operating condition contains the same number of particles (this is not always strictly true, for at times the smoke issues in a series of puffs) Equation (14) can be written:

$$N = MQ \quad (14)$$

where,

M = mass of gas per unit time passing through the engine

N = number of particles per unit time in the exhaust.

The particle concentration/unit volume, C, is:

$$C = \frac{N}{AV} = \frac{MQ}{AV} \quad (15)$$

where,

V = gas velocity (or particle velocity)

A = area of the nozzle.

Substituting this value for C in Equation (13) gives:

$$D_T = \frac{MQ}{AV} L K_2 \quad (16)$$

Rearranging the above equation to solve for Q gives:

$$Q = D_T \left(\frac{AV}{MLK_2} \right) \quad (17)$$

Substituting this value for Q into Equation (9) gives:

$$D_R = K_1 \left[D_T \frac{m}{a} \frac{AV}{MLK_2} \right]^b \quad (18)$$

Equation (18) relates the filter stain reflection density to the transmission density of the plume through the mass flow M, the area A of the nozzle, and the velocity V of the gas flow at the nozzle. This equation may be simplified if the relationship between velocity and mass flow is substituted. A reasonable assumption for velocity in subsonic flow is:

$$V = K_3 \frac{M}{A} \quad (19)$$

where K_3 is the reciprocal of the gas density. Substituting for V in Equation (18) gives:

$$D_R = K_1 \left[D_T \frac{m}{a} \frac{1}{L} \frac{K_3}{K_2} \right]^b \quad (20)$$

Equation (20) establishes the relationship between the filter stain density and the transmission density of the plume. The optical path length L is the diameter of the nozzle. The optical density is also measured at the nozzle. The mass flow M of the engine has been eliminated by the use of Equation (19).

Taking the log of Equation (20) gives:

$$\log D_R = b (\log D_T - \log L + \log m - \log a + \log K_3 - \log K_2) + \log K_1 \quad (21)$$

A simple means for testing the validity of Equation (21) would be to plot the reflection density of the filter stain D_R against the transmission density D_T of the plume on log-log paper for a series of values of Q resulting from running the engine at different power settings. The quantities m and a are held constant in the smoke sampling system as the power setting is varied. All other parameters in the equation are constant including b which is related to the retention of the filter material. If the equation is valid a straight line with slope b should result. By substituting into Equations (20) and (21) known values of all parameters and measured values of plume transmission and corresponding values of filter stain reflection density it should be possible to evaluate the constants and predict the optical transmission from the filter stain for any engine in terms of D_R and the nozzle diameter L .

(3.3.4) Relating Smoke Number to Filter Density

The smoke number is defined as:

$$\overline{SN} = (1 - \frac{R_s}{R_w})100 \quad (22)$$

where,

R_s = diffuse reflectance of the smoke spot

R_w = diffuse reflectance of clean filter paper.

Restating Equation (21), we have:

$$\frac{R_w}{R_s} = \frac{100}{100 - \overline{SN}} \quad (23)$$

or,

$$\log_{10} \frac{R_w}{R_s} = D_R = 2 - \log_{10} (100 - \overline{SN}) \quad (24)$$

where,

D_R = reflective density of the smoke stains.

Equation (24) gives the relationship between smoke number \overline{SN} and reflection density, D_R . Hence by using this value and Equations (20) or (21) it should be possible to predict the transmission of the smoke plume as a function of \overline{SN} and nozzle diameter L .

(4.) Static Tests of Engines and Aircraft

Static engine and aircraft tests were performed at NAFEC by both IITRI and FAA personnel. A number of different engines and aircraft were studied. These were: 1) a J-57-P-37A Pratt and Whitney Engine mounted on a Static, Sea Level, Open Air Test Stand; 2) a JT-12-6 engine mounted as a flight installation in a test wind tunnel; and 3) several aircraft tied-down on the National Guard run-up area at the NAFEC/Atlantic City Airport. These aircraft were an F-100, a CV-880, and a Lockheed Jetstar.

Various types of instrumentation were applied on each of the tests so that correlations between the results were possible.

(4.1) J-57-P-37A Engine Mounted in the Test Cell

The J-57 engine instrumentation consisted of an IITRI transmissometer to obtain smoke transmission data, the G.E. smoke sampler (Appendix D) to obtain smoke numbers, and the IITRI smoke sampler to obtain particle size data and smoke numbers.

Table 3 summarizes the data obtained. The transmission value reported is the one-way transmission as determined by the transmissometer and was obtained by taking the square root of the two-way measured-transmission value. The SAE smoke number is calculated as described in Appendix D. The other smoke numbers reported are variants of the SAE smoke numbers. They were obtained by substituting a Millipore filter for the standard Whatman filter or using a white backing rather than a black backing when measuring the reflectance of the filter deposits. For all power settings, no visual detection of smoke could be made by looking across the exhaust at 90° to

the jet nozzle. However, the irregular dark background of the test cell was not conducive to visible observations. Smoke could be seen only by looking along the plume path. It appeared as puffs with low obscuration values, even at the higher power settings.

Data in Table 3 show that smoke numbers collected through the IITRI probe are nearly identical to those collected through the NAFEC probe when both are located at the nozzle. Since the NAFEC probe was designed for isokinetic sampling, it is concluded that isokinetic sampling is not required for smoke number determination. Since both probes gave similar results at the nozzle, the differences between the smoke numbers obtained as the IITRI probe was moved downstream from the nozzle reflect the effect of plume dilution and expansion.

(4.2) Light Transmission of J-57 Engine Exhaust for Various Path Lengths

Visual observations of smoke plumes with both tied-down aircraft and aircraft in-flight indicated that the visibility of the smoke was dependent upon the viewing geometry. It was observed that a plume may be invisible when viewed at right angles to the plume axis, but visible as the plume was observed at other angles. The phenomena is due to the increase in the attenuation caused by the longer optical path through the plume. To illustrate this phenomena under controlled conditions, experiments with the J-57 test cell engine were conducted. The transmissometer was used to measure the light attenuated by the plume at four angles, 90° , 45° , 30° , and 19.5° , to the plume axis. These correspond to 1, 1.4, 2 and 3 times the normal (90°) path length through the plume. The engine was operated at a series of selected power settings for each angle. The results of these measurements are summarized in Table 4.

A distinct decrease in transmission as the path length through the smoke is increased is noted. If the visibility threshold is taken to be 98% transmission (see page 9) then a smoke which is invisible when viewed at 90° may become clearly visible when viewed at other angles. The results are not precise, because at the smaller angles (30° and 19.5°) it was necessary to place the corner reflector approximately 30 and 50 ft. downstream from the nozzle of the engine to protect it from the blast. The plume had become much wider at this point. Nevertheless, the principle of increased absorption with path length is clearly demonstrated.

TABLE 3
SMOKE NUMBERS AND TRANSMISSION DATA OF JET SMOKE
J-57 ENGINE MOUNTED IN TEST CELL

Test Number	Distance in Nozzle Dia. From Engine To IITRI Probe and Transmisso.	Engine Gas Flow Lbs/Sec	Engine Thrust Setting	Smoke Numbers (1)															
				G. E. Smoke Sampler								IITRI Sampler							
				Whatman Filters (2)				Millipore Filters (3)				Millipore Filters (3)				IITRI Filters (3)			
				NAFEC Probe	IITRI Probe	White Backing	Black Backing	NAFEC Probe	IITRI Probe	White Backing	Black Backing	NAFEC Probe	IITRI Probe	White Backing	Black Backing	IITRI Probe	White Backing	Black Backing	IITRI Probe
6	31	53	Idle	21	12	16	--	--	10	10	6	6	9	99.3					
7	33	94	Approach	36	27	34	25	25	26	25	21	18	68	98.4					
8	35	114	75% Norm.	49	40	48	41	41	38	37	41	40	94	96.3					
9	37	145	Cruise	55	47	54	47	47	49	48	47	46	100	95.6					
2	23	53	Idle	19	11	19	11	11	10	9	8	8	6	99.0					
3	25	94	Approach	35	26	33	24	24	24	24	20	18	30	97.3					
4	27	120	75% Norm.	50	42	42	34	34	43	42	31	30	59	95.8					
5	29	148	Cruise	58	51	--	--	--	54	53	--	--	58	96.0					
10	39	53	Idle	21	14	10	6	6	10	10	4	4	0	99.5					
11	41	94	Approach	35	27	22	15	15	24	23	13	12	9	98.1					
12	43	114	75% Norm.	48	40	34	25	25	43	42	21	20	26	97.0					
13	45	145	Cruise	55	48	39	31	31	48	46	28	27	40	95.0					
14	47	168	Takeoff	58	51	--	--	--	--	--	--	--	40	89.4(6)					

- (1) The NAFEC probe was always located at the engine nozzle. The IITRI probe was located at the distances from the engine nozzle given in column 3. All G. E. smoke sampler data were collected and analyzed by NAFEC personnel.
- (2) Whatman filter data were obtained by interpolating reflectance readings to a filtration density of $0.3 \text{ ft}^3/\text{in}^2$.
- (3) Millipore filter data were obtained by interpolating reflectance readings to a filtration density of $0.0565 \text{ ft}^3/\text{in}^2$.
- (4) The SAE smoke number.
- (5) Because the IITRI sampler filtered diluted exhaust it was necessary to extrapolate the data to a filtration density of $0.0565 \text{ ft}^3/\text{in}^2$ at thrust settings other than idle.
- (6) This value appears to be erroneous. The value of 94.2% reported in Table 4 appears more reasonable.

TABLE 4
LIGHT TRANSMISSION AS A FUNCTION OF PATH LENGTH
J-57 Engine in Test Cell

Engine Thrust Setting	Percent Transmission Relative Optical Path Through Plume ⁽¹⁾			
	1	1.4	2	3
Idle	98.2	99.0	98.9	97.8
Approach	97.0	97.0	96.4	93.0
75% Norm.	95.3	94.5	92.0	85.8
Cruise	94.3	92.4	89.0	82.2
Takeoff	94.2	91.6	88.0	79.6

(1) Relative paths correspond to angles of 90°, 45°, 30°, and 19.5° to the plume axis.

(4.3) JT-12-6 Engine Mounted in Wind Tunnel

The JT-12-6 engine instrumentation consisted of the IITRI transmissometer, GE smoke sampler, and IITRI smoke sampler. No visual or photographic observations of smoke could be made. The transmissometer was located at a distance of 7-1/2 nozzle diameters downstream from the engine nozzle and viewed the smoke plume through windows located on opposite sides of the tunnel. The IITRI smoke sampling probe was also placed 7-1/2 nozzle diameters from the engine. It was connected to the dilution apparatus by a heated sampling line. This was necessary because personnel safety considerations prevented the placement of the dilution apparatus just outside the wind tunnel at the point where the probe was placed.

Table 5 summarizes the data obtained on the JT-12-6 engine. The JT-12-6 engine gave transmission values exceeding 98% at all power settings. Based on the modeling study, this engine should not produce a visible smoke. The SAE smoke numbers were less than 25 at all power settings.

(4.4) Tied-Down Aircraft Tests

(4.4.1) F-100 Single-Engine Aircraft

An F-100 aircraft, operated by the New Jersey National Guard, was obtained for study. This aircraft has a J-57-P21A engine, similar to the engine tested in the test cell. The plane was tied-down at the National Guard run-up area at the NAFEC/Atlantic City Airport. The exhaust was analyzed with the IITRI transmissometer, the GE smoke sampler, by photographic photometry, and by visual observations. A photograph of the instrumentation is shown in Figure 3. The test results are summarized in Table 6.

The smoke numbers of the F-100 engine are similar to those obtained with the test cell engine. The smoke number at cruise is higher than at takeoff. This inconsistency is due to the movement of the aircraft at takeoff power. The nose wheel depresses and the tail of the aircraft rises at takeoff power; thus, the location of the sampling probe in relation to the engine nozzle is disturbed. The data show a distinct correlation between transmission and photographic

TABLE 5

SMOKE NUMBERS AND TRANSMISSION DATA OF JET SMOKE
JT-12-6 ENGINE MOUNTED IN WIND TUNNEL

Test Number IITRI	Engine Gas Flow Thrust lbs./sec Setting	Smoke Numbers (1)												IITRI Transmissometer (6) Percent Transmission
		G. E. Smoke Sampler												
		Whatman Filters (2)				Millipore Filters (3)				IITRI Sampler				
		NAFEC Probe		IITRI Probe		NAFEC Probe		Millipore Probe		Millipore Filter (3)		IITRI Probe		
		White Backing	Black Backing	White Backing	Black Backing	White Backing	Black Backing	White Backing	Black Backing	White Backing	Black Backing			
		White Backing	Black Backing	White Backing	Black Backing	White Backing	Black Backing	White Backing	Black Backing	White Backing	Black Backing	White Backing	Black Backing	
WT-1,2	77.78	6	4	5	4	2	3	1	2	2	1	99.1		
WT-4,5,7	80.81	29	21	14	10	21	20	8	7	1	1	98.3		
WT-6,8,9	82.83	13	25	18	12	30	29	11	10	17	17	98.1		

(1) The NAFFC probe was always located at the 12 o'clock position at the engine nozzle. The LITRI probe was always in the center of the wind tunnel 7-1/2 nozzle diameters from the engine. All G. E. smoke sampler data were collected and analyzed by NAFFC personnel.

(2) See note 2, Table 1.

() See note 1, Table 1.

(4) The SAE smoke number.

(3) See note 3, Table 1.

(4) Transmissometer located 7-1/2 nozzle diameters from engine nozzle. Path length was the diameter of the wind tunnel at this location.

TABLE 6

SMOKE QUALITY FROM A TIED-DOWN F-100 AIRCRAFT

J-57-P21A ENGINE

Engine Thrust Setting	Engine Gas Flow Lbs/Sec	II TRI Transmissometer % Transmission	Photometry (1) % Transmission	Smoke Number		Visual Transmission	
				Whatman Filter Black Backing	White Backing (2)	At Nozzle	Across Plume, % Behind Aircraft (3)
Idle	53	98	100	9	15	Clear	Clear
Approach	94	97	100	23	31	Clear	Clear
Cruise	137	95	<100	54	62	Clear	90-95 (4)
Takeoff	159	94	91-94	48 (5)	58 (5)	Clear	90-95 (4)

22

- (1) The transmissometer viewed the exhaust at the nozzle and at right angles to the direction of plume travel. The photographs were taken similarly by lying on the ground and photographing the exhaust against a sky background.
- (2) SAE smoke number.
- (3) Viewed against the normal background of the sky horizon.
- (4) Smoke is not continuous but billowy.
- (5) Low smoke numbers are attributed to the movement of the aircraft at takeoff power.



FIGURE 3. SMOKE INSTRUMENTATION.

photometry. Also, smoke with transmission values higher than 97% and smoke number values less than 23 are invisible. Smokes with transmissions less than 97% and smoke numbers above 23 are visible.

(4.4.2) Convair 880 Aircraft

The left outboard engine of a CV-880 aircraft, operated by the FAA, was studied with the same methods used for the F-100 aircraft. The engine was a CJ805-3B. Results are summarized in Table 7. The data show excellent agreement between the transmission values obtained by the transmissometer and by photographic photometry. Plumes with transmission values of 98% and SAE smoke number of 23 or less were not visible.

Conditions were ideal for photographic photometry. The plume was well above the horizon, and the sky density below the plume was essentially the same as above. For these reasons, a takeoff microdensitometer trace is shown in Figure 4. The values presented in Table 7, as well as the other tables reporting photometry data, are for the maximum decrease in optical density. For the illustrated example, this value is in the center of the plume. A positive print of the negative from which the microdensitometer trace was made is shown in Figure 5.

(4.4.3) Multiple Engines of Convair 880 Aircraft

Multiple engines of the Convair 880 aircraft were tested using the IITRI transmissometer, photographic photometry and visual estimates of obscuration. These results are summarized in Table 8. In most cases, the transmission measured photographically is less than that measured with the transmissometer. This is apparently due to ground interference with the plume. The height of the transmissometer was approximately that of the engines. The photographs, however, show the plume down to the horizon line which is well below the line of sight of the transmissometer. The microdensitometer traces, Figure 6, show a continuous increase in the density down to the horizon line. Since the obscuration values given in the tables are the maximum obscuration values (at the ground line) they will be higher than the transmissometer values because the transmissometer was fixed at the approximate average exhaust height with the engines. At the time the test was made the influence of engine tilt and ground dirt was not fully recognized.

TABLE 7

SMOKE QUALITY FROM THE NUMBER 1 ENGINE OF A TIED-DOWN CV-880 AIRCRAFT
CJ805-3B ENGINE

Engine Thrust Setting	Engine Gas Flow Lbs/Sec	IITRI Transmissometer Reading % Transmission (1)	Photographic Photometry % Transmission (1)	Smoke Number		Visual Transmission Across Plume, %	
				Black Backing	White Backing (2)	At Nozzle	Well Behind Aircraft
Idle	42	98	96	23	32	100	100
Approach	124	89	87	60	67	90-95	80-90 (3)
Cruise	147	87	85	69	73	90-95	75-85 (4)
Takeoff	163	87	86	65 (6)	70 (6)	90-95	75-85 (5)

25

(1) See note 1, Table 6.

(2) SAE smoke number.

(3) Smoke is not continuous but billowy. The smoke puffs have a transmission of 80%. Integrating the clear sky and the puffs yield an estimated visual transmission of 80-90%. Viewing the smoke from in front of the engine, the transmission varies from 40-60%.

(4) Integrated puffs and background sky give transmission values of 75-85%. When viewed from in front of the engine the transmission is 40%.

(5) Smoke is more uniform in composition, not so puffy.

(6) Low smoke numbers are attributed to movement of the aircraft at takeoff power.

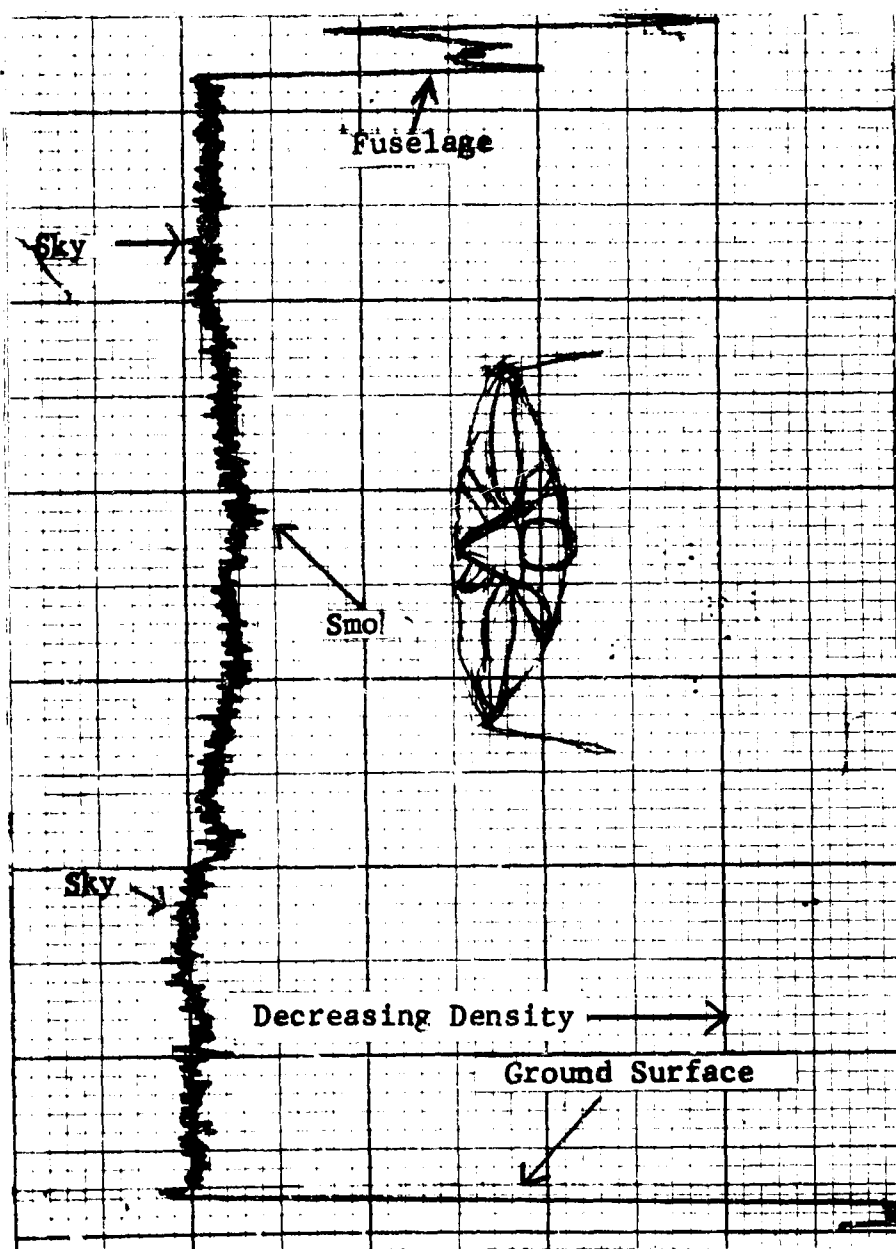
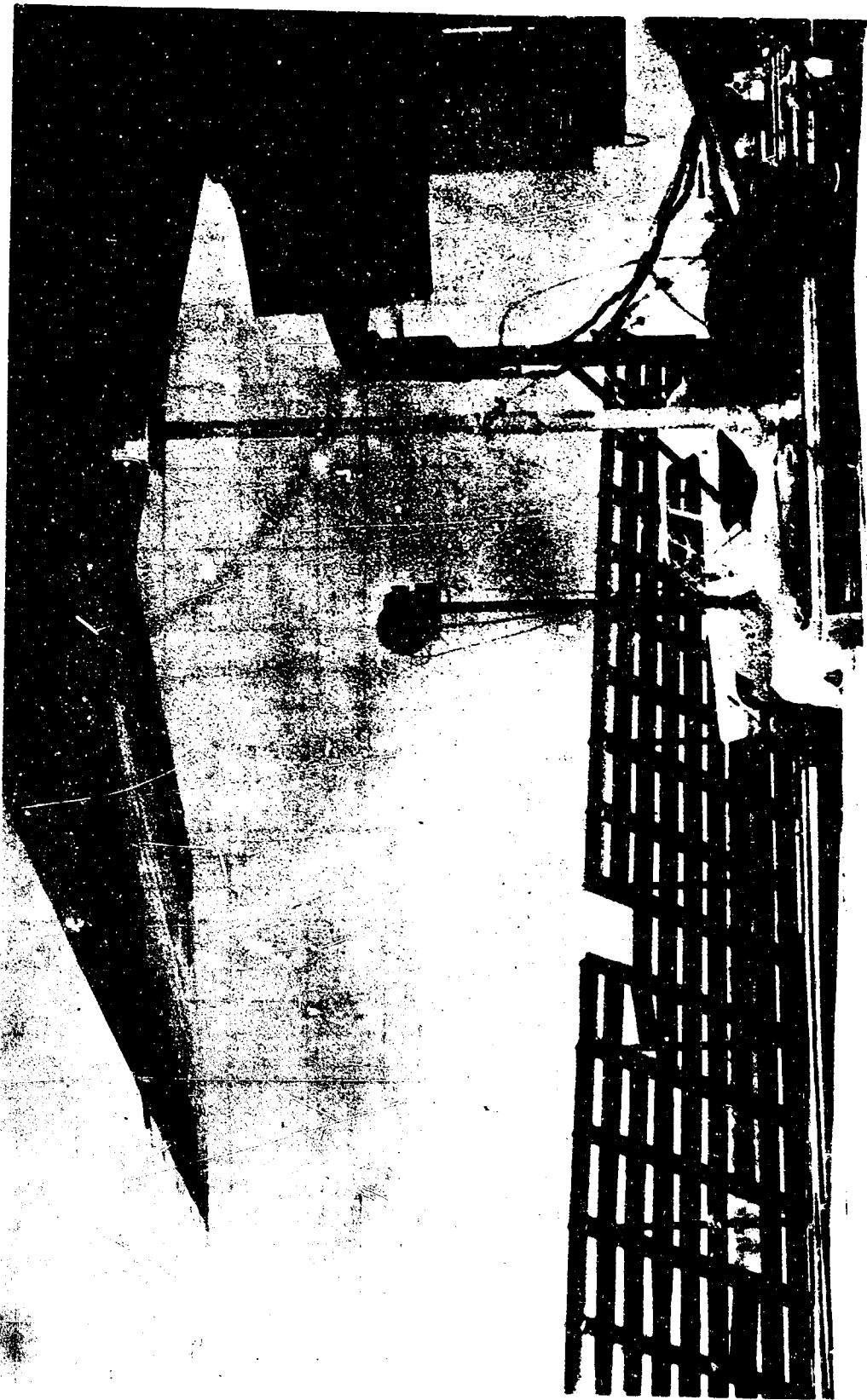
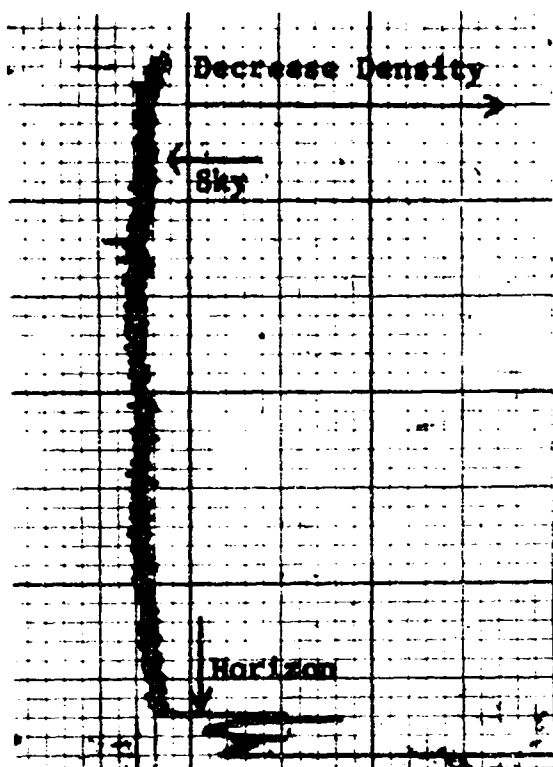


FIGURE 4. MICRODENSITOMETER TRACE OF
NUMBER 1 ENGINE OF CONVAIR 880
AIRCRAFT - TAKEOFF POWER.

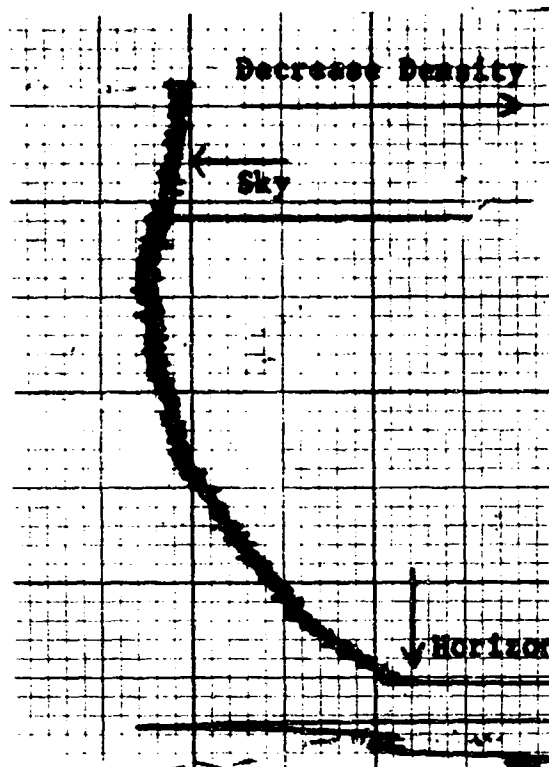


NOT REPRODUCIBLE

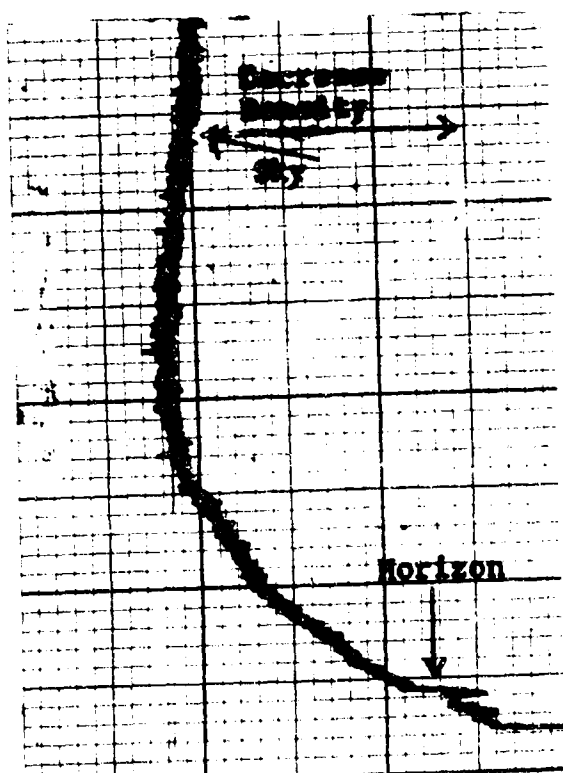
FIGURE 5. NUMBER 1 ENGINE OF CONVAIR 880 AIRCRAFT. TAKEOFF POWER.



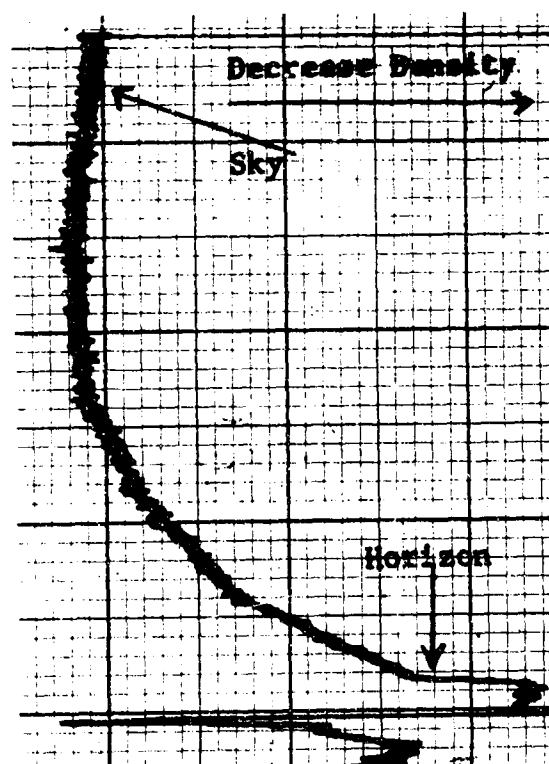
Idle Power



Approach Power



Cruise Power



Take-Off Power

FIGURE 6. MICRODENSITOMETER TRACES FROM TIED-DOWN
CONVAIR 880 AIRCRAFT - ENGINES 1, 2, and 3
OPERATING.

TABLE 8

CV-880 AIRCRAFT TIED-DOWN MULTIPLE ENGINE OBSERVATION

Engine Number in (1) Operation	Engine Thrust Setting	IITRI Transmissometer % Transmission (2)	Photographic Photometry % Transmission	Visual Transmissions % Transmission
1	Idle	99	96	100
1	Approach	91	87-94	80-95
1	Cruise	89	85	75-85
1	Takeoff	89	86	75-85
1-2	Idle	98	91	100
1-2	Approach	81	63	---
1-2	Cruise	74	49	---
1-2	Takeoff	71	49	---
1-2-3	Idle	95	95	100
1-2-3	Approach	65	49	85
1-2-3	Cruise	52	38	80-85
1-2-3	Takeoff	43	37	75-80
1-2-3-4	Idle	94	94	100
1-2-3-4	Approach	61	44	70-75
1-2-3-4	Cruise	38	28	70-75
1-2-3-4	Takeoff	30	38 (3)	70-75

(1) The number 1 engine is the left outboard engine.

(2) Transmissometer located past the tail of the aircraft at the nozzle as in previous tests

(3) It is believed that the power was being reduced when the photograph was taken.

All values obtained with either technique show a similar variation with power setting and number of engines.

The results of the multiengine study were largely nullified because of ground dirt becoming airborne during the tests. The aircraft was positioned at the run-up area with engines 3 and 4 exhausting over the ground rather than concrete. The blown ground dirt and the downward tilt of the plume is the reason why the microdensitometer traces continue to increase in density down to the horizon. However, the effect of combining smoke plumes should be predictable from consideration of increased path length.

(4.4.4) Lockheed Jetstar Aircraft

A Jetstar, owned by the FAA, was observed in the same manner as the Convair 880 aircraft. This aircraft's engine is similar to the JT-12-6 engine studied in the wind tunnel. No smoke was visible at any angle of viewing and no smoke could be detected photographically.

No transmission data were obtained with the IITRI transmissometer because of an amplifier malfunction. Repairs could not be completed in time to make the tests. Smoke numbers for the Number 4 engine were measured with the GE smoke sampler and the results are shown in Table 9.

Results show that probe location must be studied if representative smoke numbers are to be obtained. Also, a single probe location may not be a representative location for all power settings. For example, the 3 o'clock probe position gave smoke at takeoff averaging about 30% lower than the 6 o'clock position. At approach, the 3 o'clock position gave smoke numbers 25-30% higher than the 6 o'clock position. The SAE smoke numbers were below 23 at the 3 o'clock position for all thrust settings. The SAE smoke number at the 6 o'clock position reached 35 at takeoff thrust.

(4.5) Discussion and Summary of Results of Static Engine and Aircraft Tests

This discussion will show the empirical relationship between the visibility, luminance, and smoke number. Table 10 is a collection of data taken from Tables 3, 5, 6, 7 and 9, arranged to show more clearly the comparison of smoke

TABLE 9

SMOKE NUMBERS FROM THE NUMBER 4 ENGINE
OF A TIED-DOWN JETSTAR AIRCRAFT

Engine Thrust Setting	Smoke Number			
	Probe at 6 O'Clock		Probe at 3 O'Clock	
	Backing		Backing	
	Black(1)	White	Black(1)	White
Approach	8.6	12.0	10.7	15.5
Cruise	30.0	37.0	23.0	30.9
Takeoff	35.0	42.5	23.0	31.7

(1) SAE Smoke Number.

number, transmission and visibility. Figure 7 is a plot of the measured transmission against the smoke number. These values of transmission were measured at right angles at the nozzle on a single engine. As discussed on page 17, we assume that smoke with transmission values greater than 98% will be invisible. In Figure 7 a line at 98% transmission is shown to divide the plot into two parts. Above this line, the exhaust is invisible; and below the line the smoke is visible. It will be seen that SAE smoke numbers less than 23 are invisible.

A comparison between transmission measurements made with the transmissometer and with photographic photometry, Table 10, indicates that both techniques lead to similar values within experimental error. Hence, photographic photometry is a valid measure of smoke plume transmission. Photographic photometry should therefore result in true transmission values when applied to aircraft in flight.

A comparison of Columns 4 and 5 with Column 6 of Table 10 show a reasonable agreement between the transmission measurements and visual estimates of transmission.

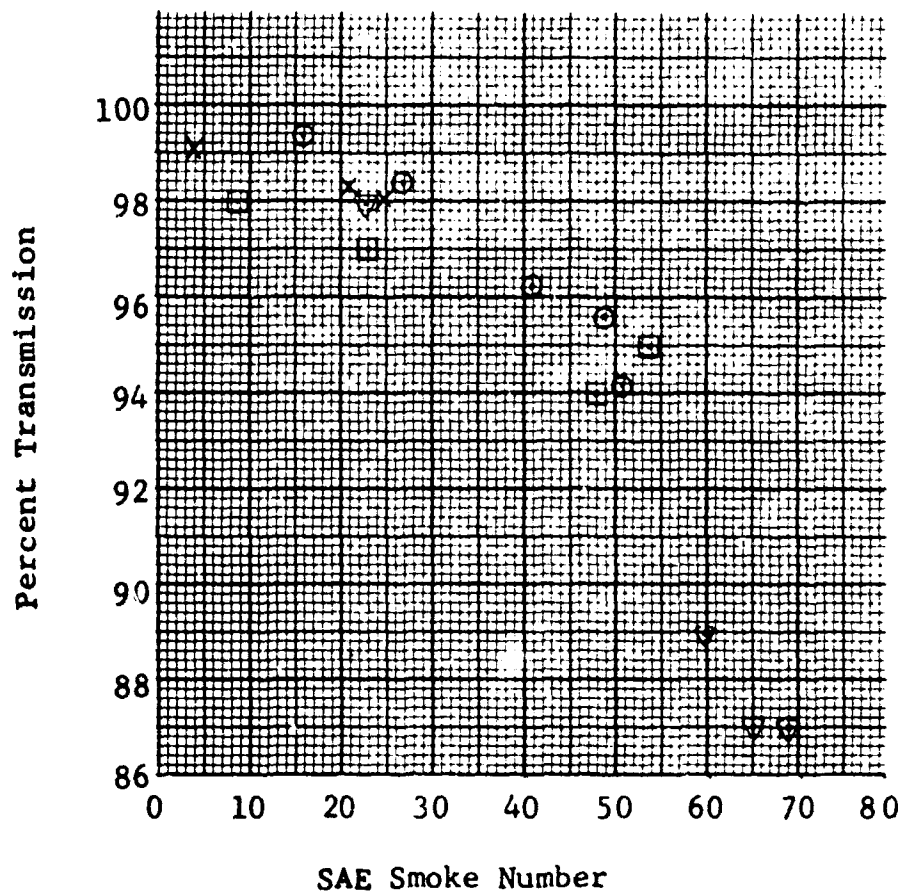
(5.) In Flight Observations

(5.1) Flights Evaluated at NAFEC

A number of different aircraft were studied in-flight at NAFEC/Atlantic City Airport, Figure 8. Photographs and visual estimates of the obscuring power of the smoke were made. The aircraft were observed during practice landing operations on runway 13-31. The observers were stationed at the junction of taxiways G and F. Aircraft maneuvers consisted of touch and go landings and takeoff or low altitude fly-bys at about 500 feet.

(5.1.1) F-100 and F-105 Aircraft In-Flight Tests

An F-100 aircraft made a number of low altitude fly-bys at several power settings with and without afterburners. A typical photograph is shown in Figure 9. Results of the visual observations and the photographic photometry measurements are given in Table 11. Two passes by an F-105 aircraft are reported in Table 12.



(All Data Taken from Table 10)

FIGURE 7. PLOT OF SMOKE NUMBER vs OPTICAL TRANSMISSION.

TABLE 10
SUMMARY OF SMOKE NUMBER
AND TRANSMISSION FOR STATIC TESTS

Engine	Engine Thrust Setting	SAE Smoke (1) Number	Transmission, %		
			IITRI Transmis-someter	Photo. Trans-mission	Visual Estim. Trans.
J-57 on Test Stand	Idle	16	99.3	--	--
	Approach	27	98.4	--	--
	75° Norm.	41	96.3	--	--
	Cruise	49	95.6	--	--
	Takeoff	51	94.2(2)	--	--
JT-12 in Wind Tunnel	Approach	4	99.1	--	--
	Cruise	21	98.3	--	--
	Takeoff	25	98.1	--	--
F-100 Tied-Down	Idle	9	98	100	100
	Approach	23	97	100	100
	Cruise	54	95	<100	90-95
	Takeoff	48	94	91-94	90-95
CV-880 Tied-Down #1 Engine	Idle	23	98	96	100
	Approach	60	89	87	80-90
	Cruise	69	87	85	75-85
	Takeoff	65	87	86	75-85
Jet-Star #4 Engine	Approach	9.8(3)	--	100	100
	Cruise	26.5	--	100	100
	Takeoff	29	--	100	100

- (1) Smoke number for black backing and Whatman #4 filters.
- (2) No data was obtained for takeoff power at the time the other test data was obtained (Table 3) due to the high noise level and vibration causing a malfunction of the voltmeter. The value shown here is from Table 4.
- (3) Smoke numbers for Jetstar are averages from black backing values at the two probe positions. See Table 9.

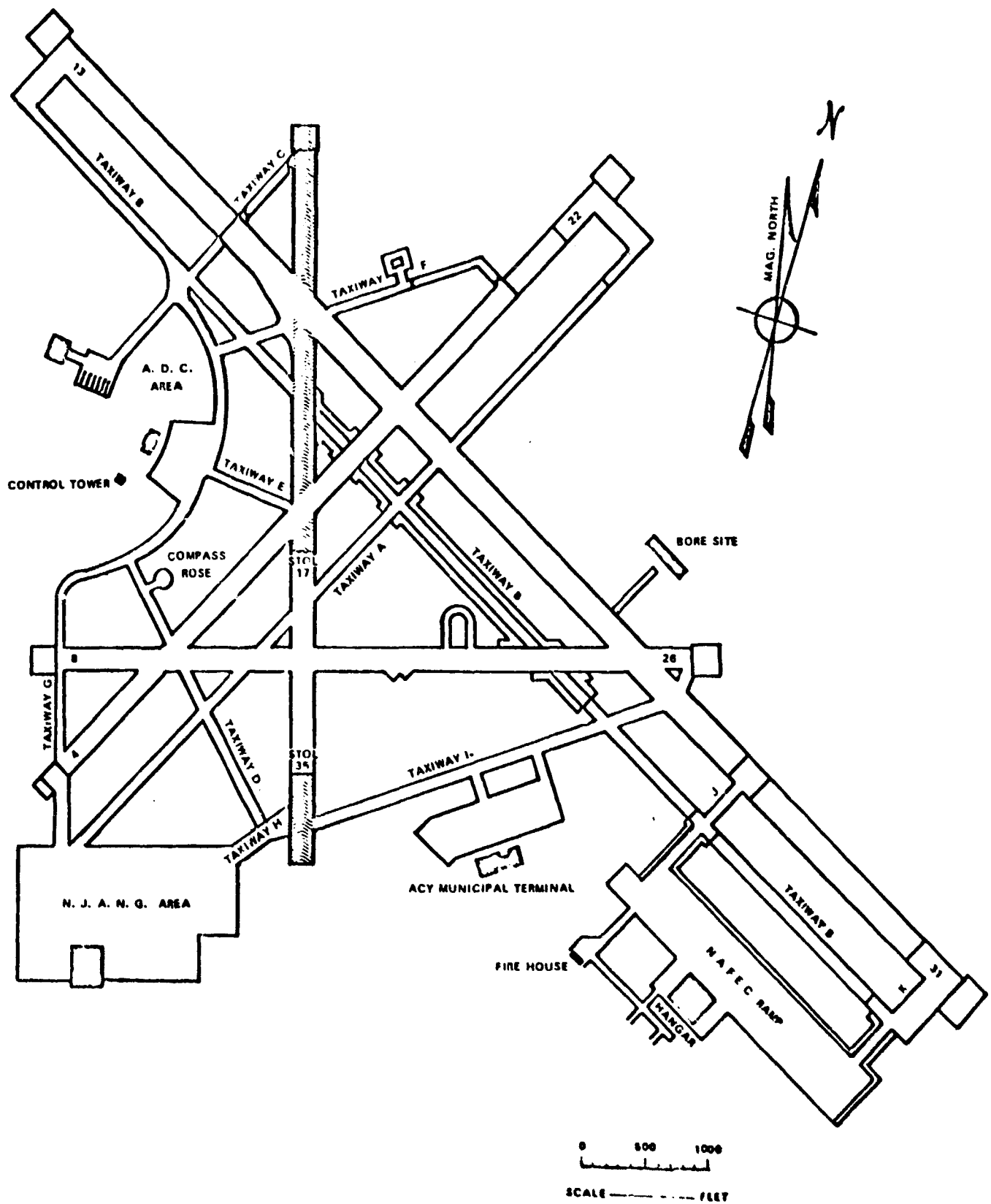
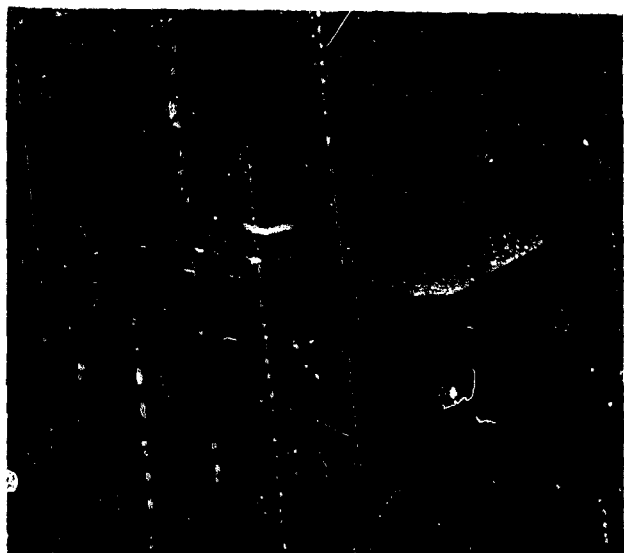


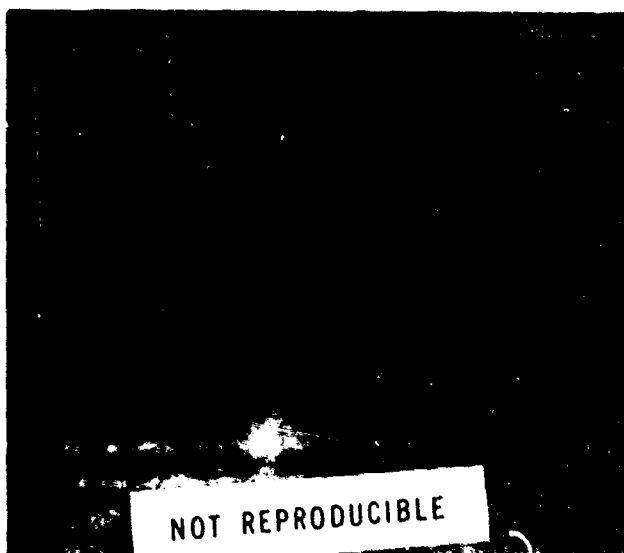
FIG. 8 NAFEC/ATLANTIC CITY AIRPORT, ATLANTIC CITY, NEW JERSEY



F-100



CV-880



CV-880



CV-880

FIGURE 9. PHOTOGRAPHS OF F-100 AND CONVAIR 880
AIRCRAFT IN FLIGHT.

TABLE 11

OBSERVATIONS ON THE F-100 AIRCRAFT IN FLIGHT AT NAFEC

Pass (1) Number	Thrust Setting	Viewing (2) Angle	Percent Light Transmission Through Plume	
			Photographic (3)	Visual (4)
1	Takeoff(5)	90°	100	100
2	Takeoff	90°	100	100
3	Military	90°	94	90
4	Military	90°	93	90
5	Cruise	90°	96	90
5	Cruise	70° (6)	92	90
6	Military	90°	96	85-90
7	Military	90°	95	85-90
8	Military	45° (7)	89	70-80
8	Military	90°	95	70-80
9	Military	30° (7)	86	50
9	Military	90°	96	80
10	Military	20-30° (7)	89	50
10	Military	90°	94	80
11	Military	30° (7)	90	50
11	Military	90°	95	80
12	Cruise	20° (7)	87	60
12	Cruise	90°	95	85
13	Cruise	10-15° (7)	80	60
13	Cruise	90°	95	85
14	Cruise	10° (6)	90	60
14	Cruise	90°	95	85

- (1) No.'s 1-7 on one film and 8-14 on other film taken on different days.
 (2) Viewing angle - angle made by line of sight and plume axis.
 (3) Transmission measured by photographic photometry (Appendix B).
 (4) Transmission as visually determined at time of flight.
 (5) With afterburner. All other data are without afterburner.
 (6) Aircraft flying away from observer, after landing exercise.
 (7) Aircraft approaching observer during landing or fly-by exercise.

TABLE 12

OBSERVATIONS ON THE F-105 AIRCRAFT IN FLIGHT AT NAFEC

<u>Pass Number</u>	<u>Estimated Thrust Setting</u>	<u>Viewing Angle</u>	<u>Percent Light Transmission Through Plume</u>	
			<u>Photographic(1)</u>	<u>Visual(2)</u>
1	Military	90°	96	85-90
2	Military	90°	95	85-90

(1) Transmission measured by photographic photometry (Appendix B)

(2) Transmission is visually determined at time of flight.

(5.1.2) Convair 880 Aircraft In-Flight Tests

Similar tests were made with the FAA Convair 880 aircraft. The data is summarized in Table 13. The data present an outstanding example of how smoke density increases as the smoke path is increased due to the position of the observer in relationship to the smoke track. When viewed at right angles visual transmission values of about 80-90% are typical. When viewed at 45°, visual transmission is on the order of 50% or less. Figure 9 shows some photographs of the CV-880 aircraft in-flight. As seen from the photographs the air during this series of flights seemed excessively turbulent.

(5.1.3) Lockheed Jetstar Aircraft In-Flight Tests

No smoke was visible to the eye and no smoke was detectable from photographs of the Jetstar. This aircraft's plume appeared clear under all conditions of viewing.

(5.2) Observations of Aircraft In-Flight at Chicago's O'Hare Airport

Table 14 summarizes the results of photographs of commercial aircraft in-flight taken at O'Hare Airport on September 25, October 23, and November 26, 1969. Most of the photographs were taken of aircraft during takeoff but a few, as noted, were taken of landing aircraft. Typical photographs are shown in Figure 10. The location of the observer relative to the plume path was far from ideal. In most instances the observer and camera were located at an undesirably long distance from the flight path.

(5.3) Discussion and Summary of In-Flight Tests

The flights observed at NAFEC show that the visual estimates of transmission are slightly lower (5-10% lower) than the photographic measurement. This discrepancy did not appear in the tied-down tests previously described and is probably due to the subjecture effect of a small plume viewed against a large expanse of light sky. Photographic transmission measurements made at 90° to the plume axis are always higher than those made at lesser angles. A similar trend may be seen in the visual estimates. Care was taken to evaluate visually the change in transmission with the viewing angle at NAFEC. The importance of this factor was not fully recognized in the earlier tests at O'Hare Airport.

TABLE 13

OBSERVATIONS ON THE CONVAIR 880
AIRCRAFT IN FLIGHT AT NAFEC

Pass Number	Thrust Setting	Viewing Angle	Percent Light Transmission Through Plume	
			Photographic(1)	Visual(2)
1	Takeoff	90°	70 & 82 ⁽³⁾	50-70
1	Takeoff	45° (5)	45	50-70
1	Takeoff	0° (5)	52 & 70 ⁽³⁾	50-70
2	Approach	45° (4)	62 & 83 ⁽³⁾	50
2	Approach	90°	81	85-90
2	Approach	5-10° (5)	44	---
2	Approach	0° (5)	70	---
3	Approach	5-10° (4)	65 & 67 ⁽³⁾	80
3	Approach	10-15° (4)	70	60-80
3	Takeoff	90°	70	80
3	Takeoff	45° (5)	44	20
3	Takeoff	20° (5)	52	30
4	Approach	0-5° (4)	44	50

- (1) Transmission measured by Photographic Photometry (Appendix B)
- (2) Visual estimate of transmission made at time of flight.
- (3) Two distinct trails appear on photograph-transmission given for each trail.
- (4) Aircraft approaching observer during landing or fly-by exercise.
- (5) Aircraft flying away from observer after landing exercise.

TABLE 14

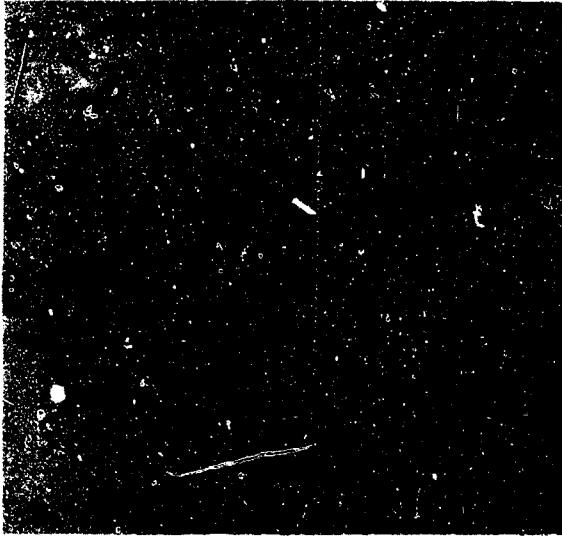
PHOTOGRAPHIC MEASUREMENT OF JET SMOKE
TRAILS FROM AIRCRAFT IN FLIGHT AT
O'HARE AIRPORT AND VISUAL ESTIMATES OF TRANSMISSION

<u>Type and Operational Mode of Aircraft(1)</u>	<u>Distance Behind Nozzle(2)</u>	<u>Number of Plumes(3)</u>	<u>Percent Light Transmission</u>	
			<u>Through Plume</u>	
			<u>Photographic(4)</u>	<u>Visual(5)</u>
727	at nozzle	1	67	25
	25 ft.	1	69	
	100 ft.	1	83	
727	at nozzle	3	83,80,84	
	75-100 ft.	2	76,82	
	100-200 ft.	1	76	
DC9	at nozzle	1	58	50
	50 ft.	1	65	
	150 ft.	1	73	
727	at nozzle	1	50	40
	100 ft.	1	73	
727	at nozzle	1	68	35
727	at nozzle	1	70	10
727*	at nozzle	1	76	30
727	at nozzle	1	74	35
707	at nozzle	1	86	70
737	at nozzle	1	100	45
727	at nozzle	2	74,83	35
727	at nozzle	1	68	30
	100 ft.	1	73	
707	at nozzle	1	86	55
	100 ft.	1	86	
	200 ft.	1	89	
2 engine	at nozzle	1	77	35

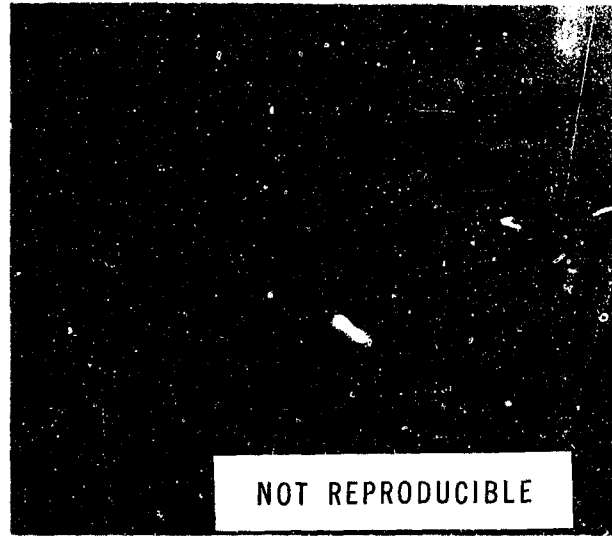
TABLE 14 (continued)

Type and Operational Mode of Aircraft(1)	Distance Behind Nozzle(2)	Number of Plume(3)	Percent Light Transmission	
			Through Plume	
			Photographic(4)	Visual(5)
2 engine	at nozzle	1	93	60
2 engine	at nozzle	1	76	20
2 engine*	at nozzle	1	73	25
DC9	at nozzle	1	76	20
DC9	at nozzle	1	75	20
727*	at nozzle	1	63	10
707*	at nozzle	1	93	85
727	at nozzle	1	73	15-25

- (1) Asterisk identifies those aircraft landing at O'Hare. All other aircraft were observed during takeoff. All aircraft are jet aircraft.
- (2) Estimated distance behind engine nozzle that the photographic transmission measurements were performed.
- (3) Number of smoke plumes at point where photographic transmission measurements were performed.
- (4) Transmission measured by photographic photometry (Appendix B). The values are for a 90° viewing angle.
- (5) Transmission as visually determined at time of light. The effect of optical path length was not fully appreciated at the time these measurements were performed. While the visual measurement was made "on mark" from the camera operator in effect the visual observer was mentally measuring the smoke density up until the time the photographs was taken. The visual transmission values therefore are not instantaneous but, integrated over a short period of time.



727 Jet - Ringelmann Number 4-1/4
September 25, 1969.



707 Jet - Ringelmann Number 3/4
September 25, 1969.

FIGURE 10. PHOTOGRAPHS OF JET EXHAUST
TRAILS DURING TAKEOFF AT O'HARE
AIRPORT.

At O'Hare, a much greater difference exists between the photographic and visual estimates. The Ringelmann reader always gave a reading equivalent to 0.75 to 1 Ringelmann numbers higher than the photographic method. These measurements were made with no previous experience on aircraft smokes and it appears that the observer tends to exaggerate the blackness of the trail against the expanse of sky. Also, the visual measurements reported were made on command from the camera operator at the time the photographs were taken. Because the smoke observer was mentally measuring the smoke density up until the time the photographs were taken the value reported is an integrated rather than an instantaneous reading. The photographic results essentially represent a plume viewing angle of 90° . However, the visual observations show the influence of viewing the smoke through greater optical path lengths prior to taking the photograph. For later measurements, the observer became more critical and was aware of great differences for various viewing angles on the same smoke trail. There appears to be no reason for demoting the photographic values in Table 14 because they agree with transmissometer data obtained under controlled conditions. Hence, the apparent difference in transmission as reported by the visual observer at NAFEC and O'Hare is due to the increased experience of the observer. It should be noted that the photographic results were not obtained until several weeks after the observations were made, so they could not influence the observer.

CONCLUSIONS

It is concluded that:

1. Considerations of turbojet exhaust visibility indicate that smoke plumes with transmission values greater than 98% will be invisible.

2. Correlations between the SAE smoke number and transmissometer data indicate that for the engines investigated, smoke numbers less than 23 are associated with invisible plumes.

3. Photographic photometry provides a means for evaluating the optical density of smoke trails from in-flight turbojet aircraft.

4. A transmissometer, of the type designed for use on this program, provides a means for evaluating the optical density of turbojet engines mounted in test cells and on tied-down aircraft. Transmission data is less sensitive than the SAE method of smoke measurement.

5. A Ringelmann smoke observer tends to overestimate the obscuration properties of jet smoke. This is believed due to several factors. Among these factors are the relative crudeness of the Ringelmann scale, the wide field of vision, the accentuated visibility of line targets, and the increase in the optical path length through smoke, when the plume is viewed at angles other than 90°.

6. Attempts to evaluate the effect of multiple plumes were nullified by ground dirt stirred up by the engine blast. However, the effect should be predictable based on theoretical considerations, as indicated by angular measurements performed on a single engine exhaust plume.

7. Jet engine smoke is composed of lacy agglomerates. The geometric median agglomerated particle size of the exhaust from the J-57 engine operated at cruise power is 0.052 μm . The geometric standard deviation is 1.46. At 10 nozzle diameters from the nozzle the geometric median size of the agglomerates is 0.13 μm .

REFERENCES

1. Aerospace Recommended Practice, ARP 1179, Smoke Measurement Techniques, Society of Automotive Engineers Inc., 2 Pennsylvania Plaza, New York, New York, 10001, Issued May 4, 1970.
2. Bureau of Mines Information Circular 7718. The Ringelmann Smoke Chart, U.S. Department of Interior, August 1968.
3. Marks, L., Mech. Engr., 59, 681, 1937.
4. Sawyer, R., Astronautics and Aeronautics, 8, 62, 1970.
5. Douglas, D., National Bureau of Standards Memo, May 20, 1954.
6. Langer, G., "The Development of Chemical Smoke Tracking Aids," IITRI Final Report C086, 1957.
7. Conner, W., Hodkinson, J., "Optical Properties and Visual Effect of Smoke Stack Plume," PHS Publ. 999-AP-30, 1967.
8. Middleton, W., "Vision Through the Atmosphere," University of Toronto Press, Toronto, Canada, 1952.
9. Horvath, H., Charlson, R., Amer. Ind. Hyg. Assoc. J., 30, 500, 1969.
10. Sallee, P. G., "A Status Report on Jet Exhaust Emissions," Air Transport Assoc. of America, 1000 Connecticut Ave., Washington, D.C. 20036, Dec. 11, 1967.
11. Dix, D., Bastress, E., "Nature and Control of Aircraft Engine Exhaust Emissions," Report #1134-1, Northern Research and Engineering Corp., 219 Vassar St., Cambridge, Mass. 02139, Nov. 1968. Report prepared for National Air Pollution Control Administration, Contract Number PH22-68-27.
12. Shaffernocker, W. and Stanforth, G. M., Smoke Measurement Techniques, SAE Air Transportation Meeting, Paper number 680346, April 29, 1968, New York.
13. Slusher, G., "Review of Investigations on Aircraft Pollution," FAA Program Review, NAFEC May 1970.
14. Mack, J. E. and Martin, M. J., "The Photographic Process" McGraw-Hill, pp. 202-204.
15. Hardy, Arthur, G., and Perrin, F. H., "The Principles of Optics," McGraw-Hill Inc., 1932, pp. 212-213.

APPENDIX A, TRANSMISSOMETER

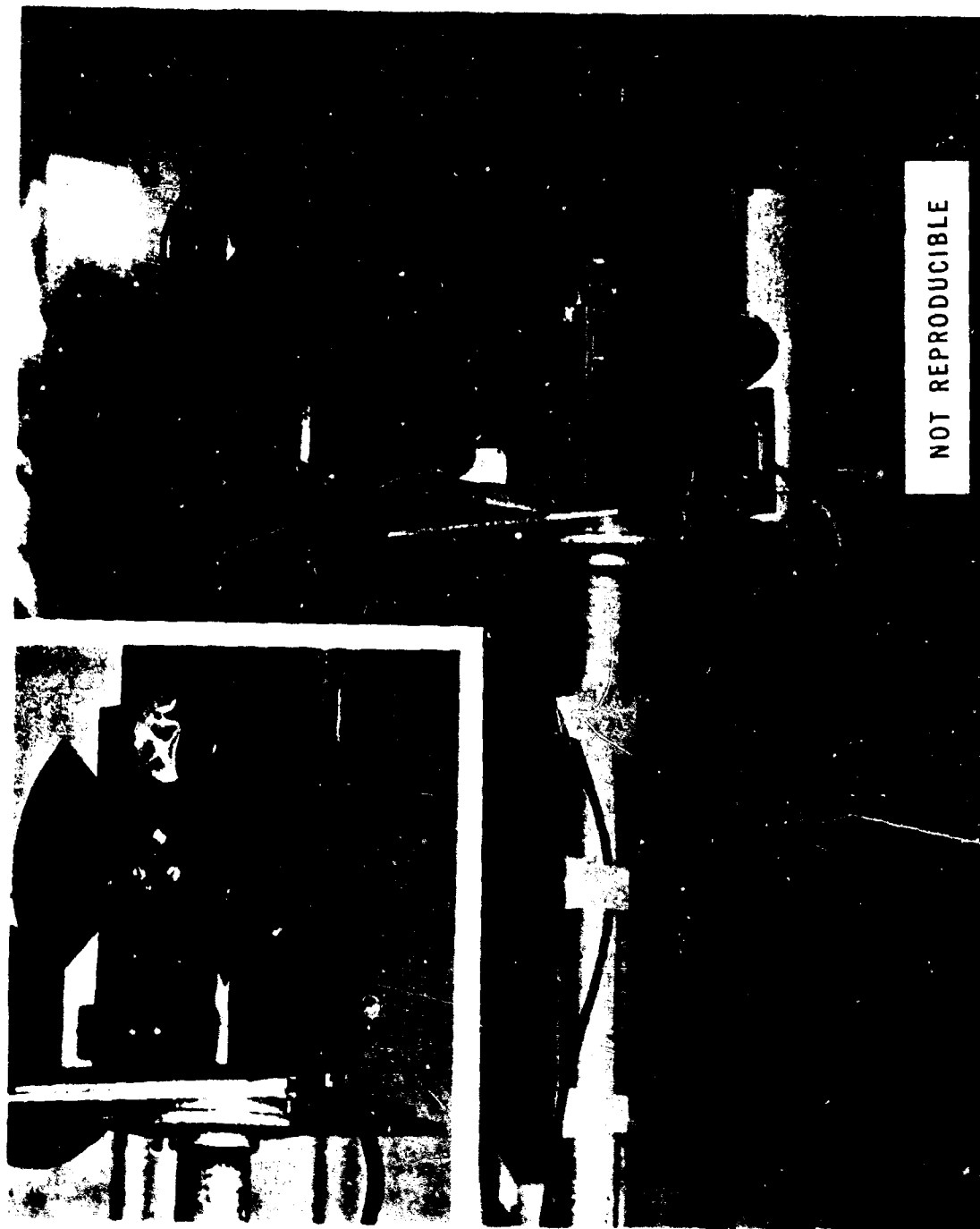
A transmissometer, Figure 1.1, was designed and constructed to measure the optical transmission of smoke plumes from jet engines under varying ambient light conditions. This transmissometer is readily portable and can operate over optical path lengths ranging from a few feet to several hundred feet without impairing its effectiveness.

A schematic optical diagram of the instrument is shown in Figure 1.2. Light from a ribbon filament lamp is focused by the condensing lens on the aperture plate and collimated by the achromatic lens. A rotating chopper, located between the condensing lens and the aperture plate, modulates the collimated beam. The beam is directed across the exhaust plume of the engine under test. On the opposite side of the plume, the beam is intercepted by a cube-corner retroreflector which directs the light back along the same path to the collimating lens. Half of the returned beam is directed to the SGD-100 silicon detector by the half-transmitting mirror. Baffles minimize the amount of light reaching the detector from scattering within the instrument. An infrared absorbing and visible transmitting filter is used to approximate visual response.

Light can reach the detector in four ways:

- (1) Light from the main beam is reflected by the corner reflector. This tranverses the smoke plume twice and is attenuated by absorption and scattering in the plume. The signal generated in this manner is the signal of interest.
- (2) Light may reach the detector from ambient light either by scattering or by directly entering the collection optics.
- (3) Light scattered in the direction of the collecting optics by particulate matter in the plume may reach the detector.
- (4) Light scattered within the instrument by lens elements, the walls of the tubes, and dust on the optical surfaces may reach the detectors.

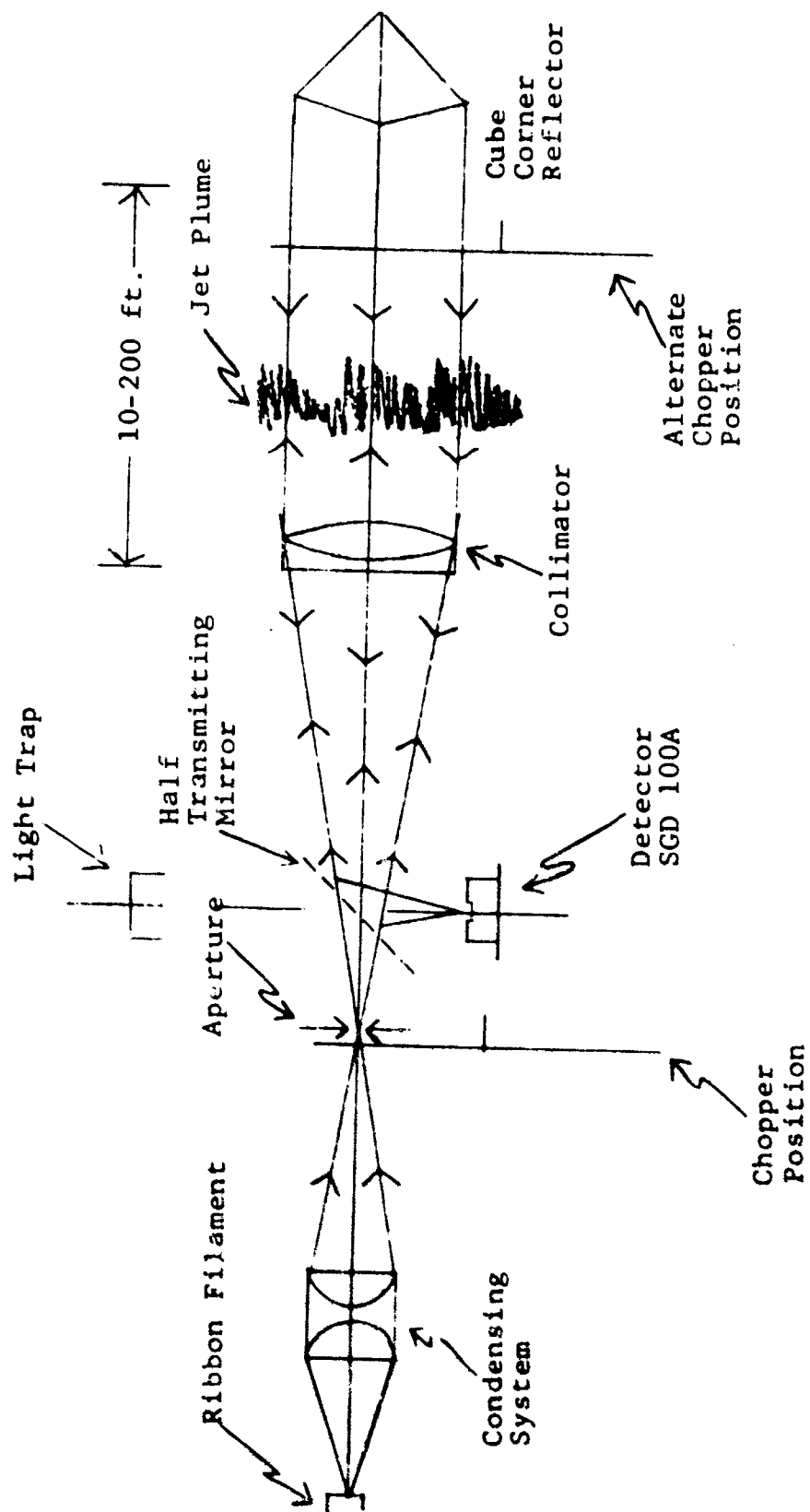
A synchronous lock-in voltmeter operating at the chopping frequency is used for signal detection. Since the ambient light is not modulated by the chopper, the ambient light gives no signal.



RETROREFLECTOR

TRANSMITTER-RECEIVER

FIGURE 1.1 TRANSMISSOMETER.



1-3

FIGURE 1.2 OPTICAL SCHEMATIC (NOT TO SCALE).

Chopped light from the beam, which is scattered back into the optics by the aerosol, as in Item 3 above, will appear as a real signal. To minimize this signal, the angular field of view is only 36 minutes of arc. By placing the chopper at the corner reflector, as shown in Figure 1.2 as the alternate chopper position, the signal contribution due to backscatter can be eliminated. By alternating the chopper position, the effect of scattering can be evaluated. In actual practice, no change in signal due to backscatter was measured, and for convenience, the chopper was used at the source position for all measurements.

Light scattered from within the instrument will give rise to an unwanted signal. However, by careful baffling and inserting a light trap above the half-transmitting mirror, error from this source was very small. At distances up to 50 feet, this signal was less than 0.1% of the signal obtained from a clear path. For distances of 150 feet or more, where the unwanted signal approached 1%, the offset-voltage-adjust on the voltmeter was used to zero out this unwanted signal. Thus, the effect of internally scattered light can be completely removed from the true signal.

Errors due to refraction by the plume are also eliminated by the instrument. The size of the projected uniform beam is larger than the retroreflector; hence, the illumination of the retroreflector remains unchanged by refraction in the plume. The return beam will retrace the same path as the projected beam so that its intensity is not affected by refractive index gradients.

The system is used to measure the transmission of smoke plumes in the following manner: the transmitter-receiver and the cube-corner retroreflector are set-up on opposite sides of the smoke plume. The light and chopper are turned on the beam centered on the retroreflector. The intensity is adjusted by a variac to give a reasonable signal. This signal is the signal corresponding to 100% transmission. The system is allowed to stabilize, and the detected voltage is recorded on a strip chart recorder. The engine under test is then started, and the signals resulting from various power settings are recorded. The two path transmission is calculated by taking the ratio of the signal to the signal obtained with 100% transmission. The square root of this ratio is the single path transmission through the plume.

APPENDIX B, PHOTOGRAPHIC INSTRUMENTATION

Photographic photometry was chosen as an objective technique for quantitatively measuring the apparent transmission of smoke plumes from aircraft in flight. If the luminance of the smoke trail and the luminance of the background upon which the smoke trail appears can be measured, then the relative luminance will give a measure of the apparent transmission of the plume. If the plume is composed of light absorbing particles that scatter light poorly then the value obtained is a true measure of the transmittance of the smoke. In actual practice, it is necessary to use the luminance of the area adjacent to the smoke plume rather than the area behind. Unless the sky is composed of small broken clouds, use of the adjacent area presents no difficulty.

While a direct reading photometer (such as small spot brightness meter or photographic exposure meter) could be used, no permanent record is available. Also, since the phenomena is transient, it is difficult to obtain reliable readings. To overcome this difficulty, it was decided to photograph the smoke trails and use photographic photometry to recover the luminance values from the photograph.

A 35 mm single lens reflex camera with 50 mm, 125 mm, and 250 mm lenses, was used to photograph the smoke trails. The longer focal-length lenses gave sufficiently large images to permit easy measurement of the density of the smoke plumes. The 125 mm proved most useful for aircraft in-flight. For tied-down aircraft, the 50 mm proved best. For measuring the density, a David W. Mann #1140 microdensitometer was used.

The technique of photographic photometry is as follows. In addition to photographing the subject whose luminance is to be measured, a transparent gray-step wedge is also photographed. When a 35 mm camera is used, the gray-step wedge is simply photographed on a separate frame from the subject. The film is then developed. Reasonable care is taken to ensure uniform development. (If a camera other than a 35 mm is used and the gray-step wedge is photographed on a separate film, care must be taken so that it receives exactly the same development time, temperature, and agitation.) In order that the film will exhibit identical response to the gray-step wedge and the subject, the gray transparent step wedge is photographed with the sky as illumination.

A convenient step wedge for calibration of the film is the Eastman Kodak Step Tablet #3, having 21 density steps ranging from 0.05 density units to 3.5 density units. The range of the step wedge is such that when the proper exposure is given, some steps are underexposed and others are overexposed.

The density of each step of the original step tablet is measured on the microdensitometer, as are the corresponding steps on the negative.

Density is defined as:

$$D = \log_{10} \frac{I_0}{I} = \log_{10} \frac{1}{T} \quad (2.1)$$

where, I_0 = the light incident on the negative,

T = the fraction of the light transmitted by the negative,

I = the light transmitted.

If the density of the negative step wedge is plotted against the logarithm of the exposure the characteristic H & D curve of the photographic emulsion results (Reference 14). (The exposure is the product of time and illuminance of the film and is commonly given in meter-candle-seconds.) It is not necessary to know the absolute value of exposure, but only the exposure ratio between the various steps of gray. From Equation (2.1), it is readily seen that the logarithm of the transmission ratio, that is, the density difference between steps of the original gray scale, is proportional to the negative logarithm of the exposure ratio for the corresponding steps on the negative. Consequently, it is convenient to plot the data for the H & D curve as shown in Figure 2.1, where the density steps of the negative are plotted against the corresponding density steps of the original gray scale.*

* The density values are measured by a densitometer depend upon the geometry of the collection optics and the light scattering of the sample as well as upon the absorption of the sample. That is, the density measured for a scattering sample by an instrument accepting a large solid angle will differ from that measured by an instrument accepting a small solid angle. The first type of instrument measures "diffuse density" and the second "specular density." A sample which does not scatter, but

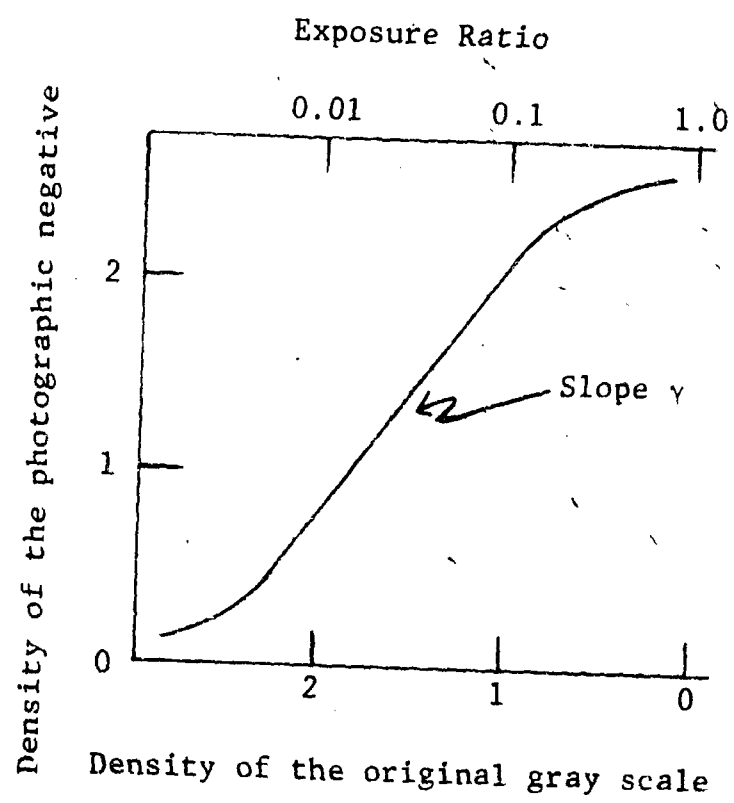


FIGURE 2.1 TYPICAL H & D CURVE.

attenuates only by absorption would give the same measurement regardless of the instrument. A photographic step wedge does scatter some light and the density will vary with the instrument used. Therefore the density as measured by the densitometer may be different than the effective density as observed by the camera and an additional step is required before the measured density differences may be expressed as log exposure ratios. The measured density may be converted to effective density by experiment as follows. A series of carefully timed camera exposures are made of the step wedge. These various timed exposures provide a series of known exposure ratios with which the measured densities of the original step wedge may be compared. In general it is found that the density values obtained by different instruments may be expressed by $D_s = g D_d$ where D_s represents the density obtained with a specular instrument (limited acceptance angle) and D_d represents the density as measured by a more diffuse instrument (large acceptance angle) and g is a constant called Calliers coefficient (Reference 15.) Calliers coefficient will be a constant depending upon the characteristics of the two particular instruments. Such an experiment was performed on the present program and it was found that density values as measured by the Mann densitometer corresponded exactly to that of the camera optics. Therefore, Calliers constant was unity and no correction was required.

If the corresponding densities of smoke plume and background on a negative are measured by a microdensitometer and compared to the H & D curve for that negative, the exposure ratio and hence, the transmission of the plume can be determined.

It is characteristic of photographic film that a portion of the H & D curve is a straight-line, thus the density difference divided by the slope of the straight-line gives the logarithm of the ratio directly. (A properly exposed negative takes advantage of this straight-line portion to correctly reproduce the relative luminances of the scene.) The slope of the straight-line portion of the H & D curve (commonly called "gamma," γ) is controlled by the development and is constant over the entire length of the film. Hence, a calibration step wedge need be photographed only once on the film. In practice, it is usually photographed at the beginning and end of the film to check on uniformity of development.

Figure 2.2 illustrates the steps in determining the luminance ratio of a smoke cloud to its background. Figure 2.2a represents a negative obtained by photographing the smoke cloud; Figure 2.2b represents the negative obtained by photographing the gray wedge; and Figure 2.2c represents an H & D plot of Figure 2.2b. The density of the steps in the gray-step negative are plotted against the density of the original step wedge. Suppose one wishes to measure the smoke luminance ratio for 2 points, a and b, in Figure 2.2a. The density of each of the points is measured and the corresponding density values plotted on the H & D curve as shown in Figure 2.2a. The corresponding original gray step wedge density difference is read from the abscissa of the curve. The density difference is equal to the negative \log_{10} of the luminance ratio.

Example: The density of point a is 1.30 (see ordinate). The density of point b is 0.99. These two points correspond to the original wedge density values a', b' of 0.75 and 1.10 (see dotted lines on Figure 2.2c.) Therefore:

$$-\log_{10} \frac{\text{luminance at b}}{\text{luminance at a}} = 1.10 - 0.75 = 0.35$$

or,

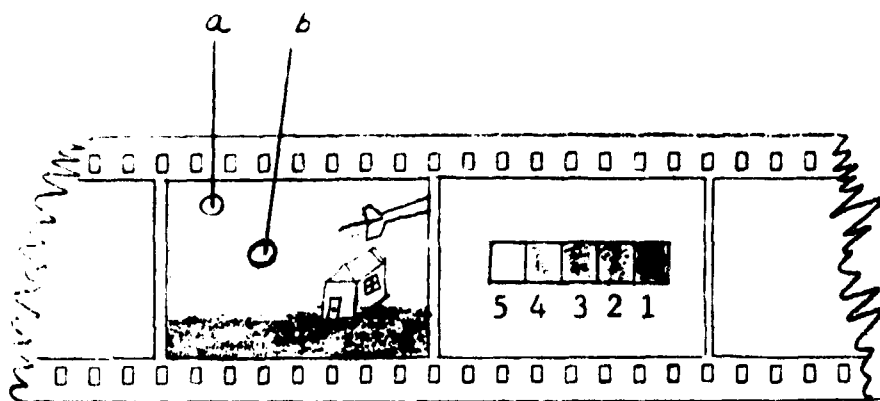
$$\log_{10} \frac{\text{luminance at b}}{\text{luminance at a}} = \log_{10} \text{ of Transmission of Smoke} = -0.35$$

Hence, Transmission of Smoke = antilog (-0.35) = 0.45 = 45%

Because the points a and b both lie on the straight line portion of the H & D curve, an alternate calculation is possible. The density difference between a and b on the negative is $\Delta D = 0.31$. The corresponding density difference on the original gray scale is:

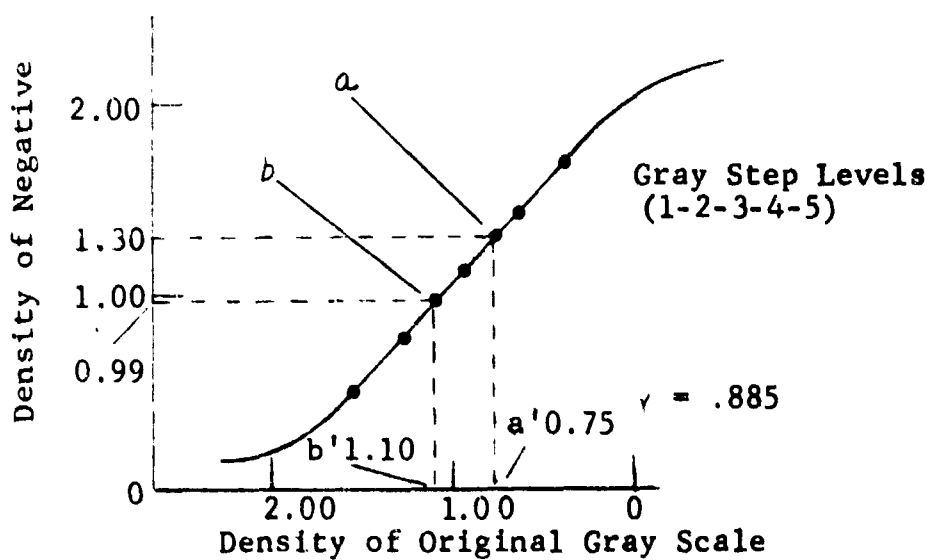
$$\Delta D' = \Delta D \times \frac{1}{\gamma} = 0.31 \times \frac{1}{0.885} = 0.35$$

Hence, $\frac{b}{a} = \text{antilog} (-0.35) = 45\% \text{ transmission.}$



a. Negative of Scene

b. Negative of Gray Stepwedge



c. H & D Curve of Negative

FIGURE 2.2 ILLUSTRATION OF USE OF PHOTOGRAPHIC PHOTOMETRY.

Note that only the luminance ratio between the smoke and the background, as seen from the observer's viewpoint, is measured. If a highly scattering medium exists in the intervening atmosphere between the observer and the plume, the observed luminance ratio will be reduced over the value at the plume. That is, contrast attenuation by the intervening atmosphere may render the interpretation inaccurate. This effect operates regardless of the type of remote observation and a Ringelmann reader is subject to the same difficulties. Hence, for reliability, observations must be made at close range and under clear air conditions.

APPENDIX C, SAMPLING JET EXHAUST FOR PARTICULATE MATTER

A special exhaust particulate sampling apparatus was used to provide a dilute sample of the exhaust gas for particle size determination. The apparatus is shown in Figure 3.1. Exhaust is drawn into the sampler by a syphon and diluted almost immediately with a large volume of cool air. A tangential inlet on the diluter facilitates mixing of the exhaust and diluent air. The cooled, diluted exhaust flows down the dilution chamber and exits at the bottom. Near the exit, samples of the diluted exhaust are collected on membrane filters and electron microscope grids. Flows to the apparatus are controlled by flowmeters. The syphon was calibrated in the laboratory prior to testing. However, the ram air effect of the exhaust invalidated the calibration and a thermoanemometer was added near the dilution chamber exit to monitor the total volume of air flowing in the apparatus. Knowing this value and the amount of syphon and dilution air, the volume of jet exhaust drawn into the apparatus was calculated. Critical orifices regulated the sample flow rate through the filters. Membrane filters were used. The instrument is shown in use at the J-57 test cell in Figure 3.2. The apparatus, with the exception of the flowmeters and pump, was placed at various distances behind the engine test fixture; the sampling probe was always located at the center of the exhaust plume. The probe was 3/8 inches in diameter.

The important features of the apparatus are enumerated below:

1. Agglomeration problems are circumvented by quickly diluting the exhaust.
2. Condensation problems are avoided by large volumes of cool diluent air.
3. Heated sample lines are not necessary.
4. Sample line deposition problems are mitigated by the use of short lines. Cleaning is facilitated.

The apparatus was used to obtain size and structure data on the exhaust particulates. Reflectance measurements were made on the membrane filters and a smoke number based on a filtration density of 0.0565 ft.³ of exhaust per in.² of filter was calculated. A white background was used during the reflectance measurement. The results, therefore, are not the SAE smoke number.

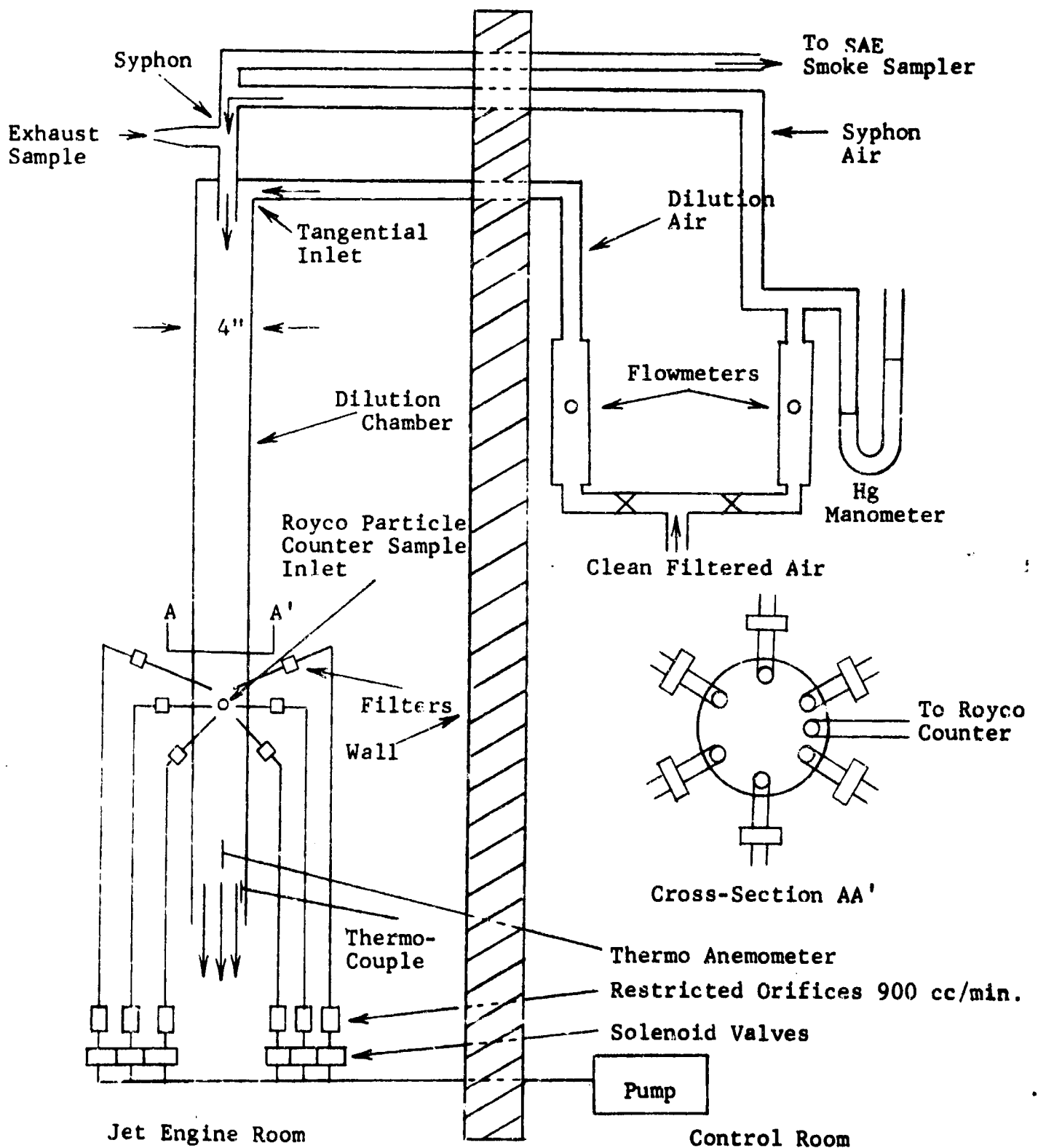


FIGURE 3.1 EXHAUST PARTICULATE SAMPLING APPARATUS.



FIGURE 3.2 IITRI SMOKE SAMPLER IN THE ENGINE TEST CELL

The diluted jet exhaust was also analyzed by a Royco Model 245 light-scattering particle counter. A 25 ft. sample line was used to connect the sampling apparatus to the Royco. The lengthy sample line was needed because the Royco is sensitive to noise and vibration; therefore, it was located in the control room. The Royco provides particle size distributions for aerosols whose particles range from 0.3μ to about 10μ . As shown in Table 2, the vast majority of smoke particles are below 0.3μ . Also, the concentration of particles, even in the diluted exhaust, exceeded the counting capacity of the Royco at all power settings, except idle. The Royco data for the J-57 engine are reported in Table 3.1.

The IITRI sampler was also used to sample the exhaust from a JT12-6 engine mounted in the NAFEC wind tunnel. The probe was placed in the center of the wind tunnel 7-1/2 nozzle diameters from the engine. Due to personnel safety considerations the dilution chamber was located in the control room and connected to the probe with a heated sampling line. Royco particle size and concentration data for the JT12-6 engine are reported in Table 3.2.

A General Electric smoke console was used by NAFEC personnel to collect samples from the IITRI sampler probe for smoke number determination. A lengthy, heated sample line, 1/4 inches in diameter, was connected to the top of the syphon for this purpose. When the smoke number was being determined, air flows to the syphon and diluter were shut off. The line to General Electric smoke console was plugged when the console was not being used.

TABLE 3.1

SIZE DISTRIBUTION AND CONCENTRATION OF EXHAUST PARTICLES
AS REPORTED BY THE ROYCO PARTICLE COUNTER-J-57-P-37A ENGINE

Test Number	Sample Location, Engine Diameters From Engine Nozzle	Engine Thrust Setting	Thousands of Particles/Ft. ³ of Undiluted Engine Exhaust					Total
			0.3-0.6 μ m	0.6-1.5 μ m	1.5-3.0 μ m	3-5 μ m	>5 μ m	
6	31	0	TMC(1)	62.2	20.7	6.9	1.9	--
7	33	0	TMC	TMC	TMC	61.7	6.2	--
8	35	0	TMC	TMC	TMC	TMC	29.8	--
9	37	0	TMC	TMC	TMC	TMC	86.3	--
2	23	2-1/2	465	260	103	2.5	1.5	832
3	25	2-1/2	TMC	TMC	TMC	13.5	4.5	--
4	27	2-1/2	TMC	TMC	TMC	23.4	4.5	--
5	29	2-1/2	TMC	TMC	TMC	TMC	38.0	--
10	39	10	385	193	43.1	7.2	4.8	633
11	41	10	TMC	TMC	201	13.4	2.2	--
12	43	10	TMC	TMC	455	36.2	2.5	--
13	45	10	TMC	TMC	TMC	84.4	6.5	--
14	47	10	TMC	TMC	TMC	249	16.6	--

(1) Too many particles to count, exceeds about 500,000 particles/ft. ³.

TABLE 3.2

SIZE DISTRIBUTION AND CONCENTRATION OF EXHAUST PARTICLES
AS REPORTED BY THE ROYCO PARTICLE COUNTER-JT12-6 ENGINE

Test Number <u>YITRI</u> <u>NAFEC</u>	Sampler Location. Engine Diameters From Engine Nozzle	Engine Thrust Setting	Thousands of Particles/ ft.^3 of Undiluted Engine Exhaust					
			0.3-0.6 μm	0.6-1.5 μm	1.5-3.0 μm	3-5 μm	>5 μm	Total
WT-1	7-1/2	Approach	270	111	16.3	1.3	0.7	399
WT-7	7-1/2	Cruise	TMC(1)	TMC	106	35.0	1.4	---
WT-9	7-1/2	Takeoff	TMC	TMC	TMC	90.0	0.3	---

(1) Too many particles to count, exceeds about 500,000 particles/ ft.^3 .

APPENDIX D, SAE STANDARD
METHOD FOR SMOKE MEASUREMENT

The Society of Automotive Engineers' Committee E-31 has developed a method for measuring and specifying turbine engine smoke. Their efforts are documented in the Aerospace Recommended Practice 1179 (Reference 1). Much of the testing required for the development of the method was conducted at NAFEC. The procedure used at NAFEC (Reference 13) involves filtering different volumes of exhaust gases and evaluating the optical density of the resulting stain. Volumes of gas, 0.1 ft^3 , 0.2 ft^3 , 0.4 ft^3 , and 0.7 ft^3 , collected in the plane of the engine nozzle were accurately measured with a wet test meter. The graduated series of stains obtained were evaluated by measuring the optical diffuse reflectance with a reflectometer. Whatman No. 4 filters are specified, but membrane filters were also used during this study to obtain comparative data. The smoke number associated with each flow is calculated from the following equation:

$$\text{Smoke Number} = \overline{\text{SN}} = \left(1 - \frac{R_s}{R_w}\right) 100 \quad (4.1)$$

where, R_s = the diffuse reflectance of the smoke deposit on the filter,

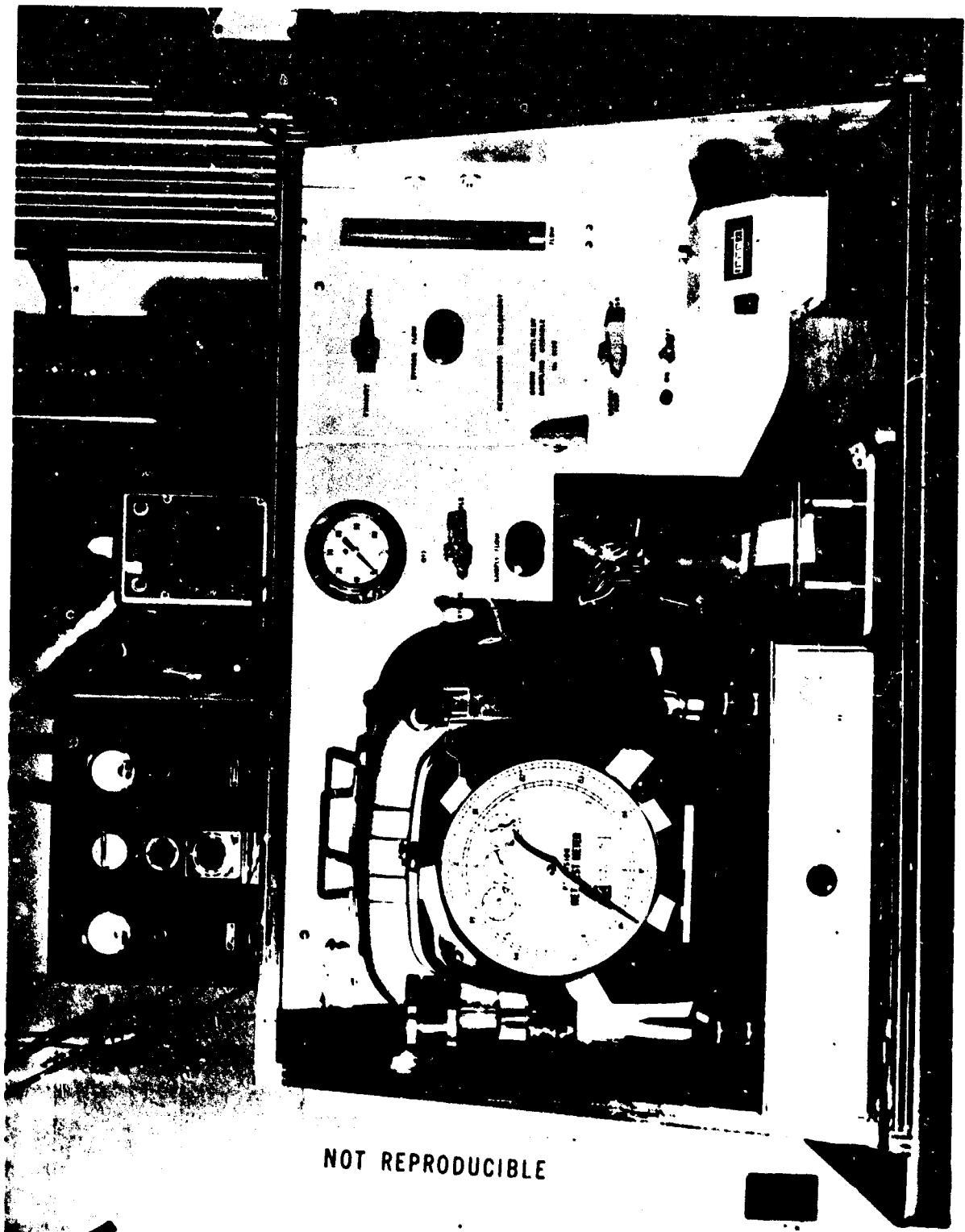
R_w = the diffuse reflectance of the clean filter.

Since R_s and R_w are functions of the material used to back the filters during analysis, the backing material must be specified. ARP No. 1179 specifies a black backing as the standard but a white backing was also used during this study. The reportable SAE smoke number is the smoke number corresponding to a gas volume of $0.3 \text{ ft}^3/\text{in}^2$ of Whatman No. 4 filter paper evaluated on a black backing. It is obtained by plotting the smoke numbers against gas volume per unit area of filter surface (log-log plot) and interpolating the curve obtained to $0.3 \text{ ft}^3/\text{in}^2$.

The probe for collecting exhaust gas is shown in Figure 4.1, installed on an F-100 aircraft. The smoke console built by General Electric and used to filter the smoke sample and measure the gas volumes, is shown in Figure 4.2.



FIGURE 4.1 F-100 AIRCRAFT WITH SAMPLING PROBES.



NOT REPRODUCIBLE

FIGURE 4.2 GENERAL ELECTRIC SMOKE SAMPLING CONSOLE.